ANALYSIS AND IDENTIFICATION OF VISUAL-MOTOR INTEGRATION IN HUMAN MOTOR CONTROL

A THESIS SUBMITTED TO
THE GRADUATE SCHOOL OF NATURAL AND APPLIED SCIENCES
OF
MIDDLE EAST TECHNICAL UNIVERSITY

BY

AYŞEGÜL KILIÇ

IN PARTIAL FULFILLMENT OF THE REQUIREMENTS
FOR
THE DEGREE OF MASTER OF SCIENCE
IN
ELECTRICAL AND ELECTRONICS ENGINEERING

SEPTEMBER 2023

Approval of the thesis:

ANALYSIS AND IDENTIFICATION OF VISUAL-MOTOR INTEGRATION IN HUMAN MOTOR CONTROL

submitted by **AYŞEGÜL KILIÇ** in partial fulfillment of the requirements for the degree of **Master of Science in Electrical and Electronics Engineering Department, Middle East Technical University** by,

Prof. Dr. Halil Kalıpçılar
Dean, Graduate School of **Natural and Applied Sciences** _____

Prof. Dr. İlkay Ulusoy
Head of Department, **Electrical and Electronics Engineering** _____

Assist. Prof. Dr. Mustafa Mert Ankaralı
Supervisor, **Electrical and Electronics Engineering, METU** _____

Examining Committee Members:

Prof. Dr. Afşar Saranlı
Electrical and Electronics Engineering, METU _____

Assist. Prof. Dr. Mustafa Mert Ankaralı
Electrical and Electronics Engineering, METU _____

Assist. Prof. Dr. İsmail Uyanık
Electrical and Electronics Engineering, Hacettepe University _____

Date:11.09.2023

I hereby declare that all information in this document has been obtained and presented in accordance with academic rules and ethical conduct. I also declare that, as required by these rules and conduct, I have fully cited and referenced all material and results that are not original to this work.

Name, Surname: Ayşegül Kılıç

Signature :

ABSTRACT

ANALYSIS AND IDENTIFICATION OF VISUAL-MOTOR INTEGRATION IN HUMAN MOTOR CONTROL

Kılıç, Ayşegül
M.S., Department of Electrical and Electronics Engineering
Supervisor: Assist. Prof. Dr. Mustafa Mert Ankaralı

September 2023, 71 pages

This research focuses on the complexities of visual-motor integration in humans using target-tracking tasks, emphasizing the dynamics of human-in-loop systems. Drawing from the foundations of the pursuit and compensatory control models, the study accentuates the profound influence of feedback mechanisms and the predictability of inputs on performance outcomes.

The research design included four distinct target-tracking tasks, each examining different aspects of visual-motor integration. These tasks were characterized by variations in trajectory types, including single-frequency sinusoids and sum-of-sine, and differences in experimental scenes, ranging from visibility of the target and operator to only error information representation. We collected 25 participants' position and velocity data with a haptic device.

An accurate response was observed when participants received direct visual feedback even under unpredictable stimuli. Another observation was the overall better tracking performance when the input was predictable compared to unpredictable stimuli.

Also, we compared the performance enhancement created by the input and feedback. We saw that increasing the predictability of the input was more effective than increasing the feedback supplied to improve the performance. Moreover, the consistent emergence of a "U" shaped magnitude response across unpredictable input experiments alludes to potential intrinsic properties of the human motor system, possibly influenced by factors such as neural resonance.

This research integrates conventional methodologies with more realistic scenarios, offering a layered and more nuanced understanding of human capabilities and limitations in motor control models and opening up opportunities for designing systems that can better interact with or augment human abilities.

Keywords: human manual target tracking, visual-motor integration, input predictability, feedback predictability, system identification

ÖZ

İNSAN MOTOR KONTROLÜNDE GÖRSEL-MOTOR ENTEGRASYONUNUN ANALİZİ VE TANIMLANMASI

Kılıç, Ayşegül
Yüksek Lisans, Elektrik ve Elektronik Mühendisliği Bölümü
Tez Yöneticisi: Dr. Öğr. Üyesi. Mustafa Mert Ankaralı

Eylül 2023 , 71 sayfa

Bu araştırma, hedef takip görevlerini kullanarak insanlarda görsel-motor entegrasyonun karmaşıklığına odaklanırken insanın sistemin içinde olduğu durumların dinamiklerini göz önünde bulundurur. Takip ve telafi edici kontrol modellerinin temellerinden yola çıkan bu çalışma, geri bildirim mekanizmalarının ve girdilerin öngörülebilirliğinin takip performansı üzerindeki temel etkilerini öne çıkarmaktadır.

Araştırma tasarımı, görsel-motor entegrasyonun farklı yönlerini inceleyen dört farklı hedef takip görevini içermektedir. Bu görevler, tek frekanslı sinüzoidler ve toplam sinüzoidler gibi yörünge türlerinde varyasyonlar ve hedefin ve operatörün görünürlüğünden sadece hata bilgisi temsiline kadar değişen deneysel sahnelerle karakterize edilmiştir. 25 katılımcının pozisyon ve hız verileri bir haptik cihazla toplanmıştır.

Katılımcıların doğrudan görsel geri bildirim aldığında, öngörülemeyen uyaranlar altında bile isabetli bir tepki verdiği gözlenmiştir. Başka bir gözlem ise, girdi öngörülebilir olduğunda izleme performansının, öngörülemeyen uyaranlara kıyasla genel olarak daha iyi olduğu yönünde olmuştur. Ayrıca, girdi ve geri bildirimin oluşturduğu

performans artışları karşılaştırılmıştır. Girdinin öngörülebilirliğini artırmanın, performansı iyileştirmek için sağlanan geri dönüşü artırmaktan daha etkili olduğunu görülmüştür. Ayrıca, öngörülemeyen giriş deneylerinde tutarlı bir şekilde "U" şeklinde büyüklük tepkisinin ortaya çıkmasının, insan motor sisteminin potansiyel içsel özelliklerine işaret ediyor olabileceği, bunun da nöral rezonans gibi faktörler tarafından kaynaklandığı düşünülmektedir.

Bu araştırma, geleneksel uygulamaların üzerine daha gerçekçi senaryolar entegre ederek motor kontrol modellerinde insanın yetenekleri ve sınırları hakkında katmanlı ve daha ayrıntılı bir anlayış sunar. İnsan yetenekleriyle daha iyi etkileşimde bulunan veya yeteneklerini artıran sistemler tasarlama fırsatları sunar.

Anahtar Kelimeler: insan manuel hedef takibi, görsel-motor entegrasyonu, girdi öngörülebilirliği, geri bildirim öngörülebilirliği, sistem tanımlama

To my beloved family

ACKNOWLEDGMENTS

First and foremost, I would like to express my sincere gratitude to my supervisor, Assist. Prof. Dr. Mustafa Mert Ankaralı. His continuous support, encouragement, and guidance throughout these three years have been invaluable. Being under his mentorship and benefiting from his knowledge has been a great experience in my academic journey.

I want to thank Osman Kaan Karagöz, a great friend and a mentor, who was there when the workload - or food - seemed like a mountain. My friends, especially Pınar Cemre Yazıcı, Oğuz Kağan Üre, and Utku Elagöz were a phone call away when life got tough. Thank you all for your endless support. I could not made it without any of you.

Most importantly, I would like to express my deepest gratitude to my family. This thesis would not have been possible without them. My mother, Zeynep Kılıç and my father, İsmail Kılıç were always there for me and supported me in every possible way. I cannot thank them enough for all their love and sacrifices. I want to thank my sister Pelin, who is also my best friend, the mother of my favorite person, and perhaps the most influential person in becoming who I am now. My dearest niece, Nil, you are the very best thing that ever happened to our family. Thank you for being our sunshine and joy in life.

I am thankful for the financial support from the National Scientific and Technological Research Council of Turkey (TÜBİTAK) through the 2210 M.S. scholarship program.

TABLE OF CONTENTS

LIST OF TABLES

TABLES

LIST OF FIGURES

FIGURES

LIST OF ABBREVIATIONS

ABBREVIATIONS

SoS	Sum-of-Sines
SS	Single Sine
1D	1 Dimensional
MSE	Mean Squared Error
FFT	Fast Fourier Transform
IMP	Internal Model Predictor

CHAPTER 1

INTRODUCTION

1.1 Motivation and Background

The movement of animals is a complex phenomenon that arises from the dynamic interaction between their motor and sensory systems. The ability to maintain stability and accuracy during movement is crucial for an animal's survival, as it ensures prey does not stumble or fall while being pursued by predators, while the predators rely on their tracking ability to sustain.

It is common to use feedback control as a framework to understand the dynamic under these movements [1, 2, 3, 4], as it offers structured insights into the dynamic interplay between sensory feedback and motor responses. The literature offers examples ranging from the walking analysis of humans [5] to the examination of the effect of locomotor dynamics variability of glass knifefish [6]. Motor behaviors can be represented as closed-loop systems. In this conceptualization, bodily movement is achieved by activating the musculoskeletal components. In turn, this movement stimulates the sensory systems. Neural components respond to sensory inputs, modify motor activations, and complete the loop.

Control theory typically models closed-loop systems with three main components: the controlled (plant), the controller, and the feedback. In the realm of animal movements, the musculoskeletal components are perceived as the plant [7], and the neural components serve as the controller [2, 8, 9] respectively, with sensory stimuli acting as feedback. The nervous system, for the majority of animals, receives sensory feedback from various sources that shape a distinct motor response suitable for the intended action. Sensory feedback can manifest as visuals, tactile sensations, auditory

cues, and vestibular signals, among others.

Within this framework, the neural components of the body address two primary concerns: state estimation and control strategy. State estimation problem is an attempt to understand the current conditions of a system, such as body orientation relative to itself and its surroundings. Enhanced state estimation performance allows precise adjustments, optimizing the movement. The control strategy is created using estimated states to modulate muscle activation levels accordingly, ensuring coordinated and efficient locomotion, as observed in Hummingbird's case [10].

As mentioned earlier, there are several feedback sources, and sensory stimuli often reach the nervous system as a combination of different feedback signals from different sensory systems of the body. Studies have explored haptic feedback in tasks like juggling [11] and have delved into the significance of vestibular feedback [12]. Among these, visual feedback stands out. The nervous system places significant emphasis on visual cues regarding state estimation and the control decision processes during motor tasks for most animals.

Visual-motor integration, the cognitive ability to incorporate visual feedback into motor behavior, enables successful execution of body movements. We can find evidence from nature that proves this point. The hawkmoth *Manduca sexta's* [13] and the weakly electric fish *Eigenmannia virecens'* [14] natural tracking behaviors, for instance, are influenced by the luminance of the environment. Additionally, while preying, bluefish's prey tracking ability is primarily dictated by visual feedback [15].

Tracking is a universal trait observed in animals, driven by needs like predation, mating, or foraging. Similarly, as humans, we also engage in various tracking tasks. Whether it is pilots tracking targets in military operations [16, 17], surgeons leveraging joystick-like controllers in robotic surgeries utilizing the visual feedback to achieve precision in intricate procedures [18, 19, 20], or even in entertainment, while playing video games which often require players to track and engage moving targets on screen [21, 22], emphasizing the ubiquity and importance of tracking in our lives. This research aims to investigate the isolated influence of visual feedback on human motor movements during tracking tasks, distinguishing its effects from other sensory inputs.

1.2 Biological Review

Human's central nervous system, composed of various units, serves as the body's command center. It is designed to adjust to both internal and external changes consistently. This intricate system preserves posture, facilitates movement, and offers fine motor control [23].

Also, our body is designed to move in the best way possible. It integrates principles like balance and momentum to do activities efficiently. For example, this optimization helps us walk easily without getting tired quickly. For example, when we walk, our legs go through cycles of supporting our weight and swinging forward. This way, only some muscles are working hard at any one time, which helps us keep going without getting tired. [24].

When it comes to moving on purpose, like lifting your arm, it all starts in the brain. The messages from the brain first go to a part called the cerebellum before telling the muscles what to do. The cerebellum is the protector of balance and fluidity in muscular activities. Then, these messages are sent to the muscles to get them moving. As we engage in a motion, our brain continuously harvests real-time data on body orientation, making micro-adjustments in the blink of an eye. If something goes off course, the cerebellum corrects it quickly. Thus, any damage to the cerebellum can disrupt this harmony, resulting in imprecise and rough movements.

The cerebellum also helps us get better at tasks we do repeatedly, like riding a bike, taking a role in learning and adaptation. At first, movements are rough and less stable, but with more practice, they become smoother. This improvement happens because the cerebellum strengthens the brain pathways needed for the task [25].

1.3 Existing Works

The question of how animals utilize their senses in varied tasks has been a subject of curiosity and research since the dawn of humanity. The fact that many animals are equipped with multiple senses, which they deploy in distinct ways for specific actions, has broadened this research field.

Most real-life tasks of animals require several sensory feedback pathways rather than dependence on just one. In the research presented in [11], Ankaralı *et. al.* explores the impact of haptic feedback on rhythmic behaviors by comparing two paddle juggling tasks – one with visual feedback and the other with visual and haptic feedback. Similarly, Nickl *et al.* [26] examines the effect of audio and haptic feedback when combined with visual feedback. Roth *et al.* [27] provide a framework for stimulating and modeling various senses in multisensory behaviors, using the hawkmoth's flower-tracking behavior as a case study.

Vision often stands out as the most fundamental and pivotal sense of all the senses. Spanning a wide range of species, from the most primitive to the most advanced, is one of the main focuses of research to understand the relation between sensory perception and task performance. We can see many visuomotor control analysis and modeling examples for humans, whether it focuses on the task of pole balancing on a finger [28] or how it can be improved by action video games [29].

We can use tracking tasks to look into several aspects of visuomotor control. Human target tracking, deeply rooted in the challenges of human-machine control in aircraft systems [30], has evolved over the years. McRuer *et al.* [31] formulated a human target tracking task with three levels depending on the predictability of the input and skill improvement ability of the operator. In the compensatory control level, tracking error is the only feedback, and tracking performance relies heavily on this feedback. McRuer's crossover model [32] captures the compensatory control and models the plant and the operator together as an integrator with a delay. The second level is pursuit control, which applies when the operator has past experience, creating an expectation for the input's future. However, correction of the response is completed with the help of visual feedback. The highest level is precognitive control, where the operator knows the input's entire future.

In the pursuit control level, the operator is hypothesized to use feedforward control along with the feedback control [32, 33, 34, 35]. McRuer *et al.* [33] hypothesize that the compensatory case's control corresponds to the feedback controller of the pursuit control, and the feedforward component can be assumed as the inverse of the controlled dynamics. In research presented in [34], a disturbance signal is introduced

to the task to identify the control components, and similar to the previous work, the feedforward component is modeled similarly to the inverse system dynamics. This has become a common assumption and an outcome for the upcoming research in the ongoing years [36]. Roth *et. al.* [37] investigates the measure of the ability of the operator to learn and invert the controlled dynamics. Yamagami *et. al.* [38] suggests that this inversion is applicable at lower frequencies, yet they find this assumption not applicable to higher frequencies and define a frequency limit to this inversion.

The recent study presented in [39] proposes an identification method to simultaneously estimate the feedback and feedforward controllers of the pursuit control by introducing a disturbance signal and applying FFT with a Hanning window on both the disturbance and output signals.

[40] compares the tracking performances of humans on horizontal and vertical axes and suggests better performance on the horizontal axis. In a similar study to understand the human's capabilities, Yamagami *et. al.* investigates the control strategy differences between using their dominant versus nondominant hand [41], yet do not detect any significant differences. Also, in [42], they use an electromyography (EMG) interface as an alternative to joystick-like interfaces. They found that EMG improves the user's reaction time and more significant bandwidth, which could be helpful in multimodal interfaces.

The predictability of the input creates another research question. In [43] Yang *et. al.* use a complex tracking task that requires continuous adjustments of motor control to understand how people learn and adapt to perform under unpredictable scenarios. Similarly, [44] delves into which characteristics make the system difficult to control. [45] proposes a method to compensate for the delay caused by the unpredictability nature of the input. This question is also investigated for weakly electric glass knifefish in [46] using single sine, and sum-of-sines signals as a trajectory for fish to follow.

1.4 Contributions

To evaluate the impact of visual cues on tracking motor performance, we designed a simple one-dimensional manual target-tracking environment in virtual reality. We

created four fundamental experimental scenarios with two types of experimental scenes and two types of target trajectory inputs. Changing them one by one, we aimed to create a controlled experiment series and distinguish the effects of each change on the target tracking performance.

Inspired by the work of [31], we delved into two specific visual notification-based scenes in our experiments. In the first two experiments, we created a scene to replicate the pursuit tracking control, allowing participants to see the input, the target object's position to be followed, and the output, which is the subject's position. The only change between the first two experiments is the input form, one being a single sine trajectory repeated for multiple frequencies and the second being a special sum-of-sines trajectory. On the other hand, the third and fourth experiments are build upon the second scene, which mimics the compensatory tracking control introduced in the same research. In this scene, only the difference between the target's and the subject's position, that is, error information of the position, is given to the subject. Again, we changed the input form as in the first and second experimental scenarios. Combined with the exploration of multiple inputs, these scenarios offered a layered understanding of human tracking behavior under the influence of distinct visual cues.

In this work, creating the compensatory tracking scenario is our principal contribution. Even though the pursuit task is discussed in many papers [39, 34, 32], to the best of our knowledge, the compensatory case has yet to be created as an experimental scenario. By creating this environment, we formed a basis to investigate the zero-input conditions without an assumption. We also take the visual feedback created unintentionally by participants' seeing their own hands while performing the given tasks into consideration and make sure to eliminate it by using the experimental setup and giving instructions to participants, which will be further discussed in the following chapters.

We aim to investigate the effect of input predictability on the tracking performance of a pursuit tracking task by comparing the first two experiments. On the other hand, input predictability's change on the tracking performance of a compensatory system is made by comparing the last two experiments. We also mention the comparison of pursuit tracking and compensatory tracking by comparing both single-sine experiments

in two different scenes. We create our last and most complex analysis by comparing two different experimental scenes with sum-of-sines input, which makes it harder to interpret the effect of unpredictabilities introduced by two different sources.

In situations where an individual's tracking performance is crucial, such as if the operator is a pilot or a surgeon, it is vital to measure and improve their abilities before assigning them significant tasks. Examples of this can be seen in publications about enhancing skills in using surgical robots, as in [47] is important for the operation's success. Also, it has been observed that virtual environments are successful in improving and optimizing these skills [48], [49]. The experimental environment we have created not only quantifies an individual's abilities but also provides a medium in which these skills can be developed and enhanced. By employing VR, we have presented a controlled and immersive environment. Our setup replicates real-world challenges authentically and eases the analysis of understanding the impact of visual cues.

Compared to the previous works in the related field, this research is conducted with an impressive number of 25 participants with a higher demographic variability of almost half and half division between the genders.

To sum up, our research enlightens visual cues' significant role in tracking motor performance. The domain of human tracking performance has been rich with research, particularly around human-machine dynamics and tracking patterns. By harnessing the capabilities of virtual reality and examining different visual scenarios, we have added a nuanced dimension to the ongoing conversation in this field, with potential real-world applications in sight.

1.5 Organization of Thesis

In Chapter 2, we provide an in-depth description of the apparatus details, the experimental setup, the experimental scenarios, the experimental sequence, and the instructions imparted to participants. We finish this section with the data collection techniques that we used.

Later in Chapter 3, we define the performance metrics for the tasks and explain the methodology we used to identify and analyze the system.

In Chapter 4, we investigate the results of each experiment individually and compare the findings. Then, we try to emphasize the possible reasons underlying the difference between the results and give our hypotheses.

Finally, in Chapter 5, we conclude this work with a summary of the key findings and mention possible future work.

CHAPTER 2

EXPERIMENTS

In this chapter, we meticulously outline the methodological framework employed to probe the intricacies of visual-motor integration in human subjects. Central to this investigation is the role of visual feedback in guiding motor responses. The chapter provides an in-depth description of the apparatus used, the experimental setup, calibration procedures, and the instructions imparted to participants. Furthermore, it details the structured sequence of experiments, data collection methodologies, and the analytical tools employed. Ethical considerations, essential to uphold the research's integrity, are also given in this chapter. By presenting a thorough account of the experimental process, this chapter ensures transparency and lays the foundation for potential replication in future studies centered on visual-motor integration.

This study was approved by the Human Subjects Ethics Committee at Middle East Technical University with the protocol number 0505-ODTUIAEK-2022. A total of 25 participants, comprising 11 females and 14 males, participated in the experiments. Their ages ranged between 20 and 30 years. We only recorded their gender and refrained from collecting any other personal details.

2.1 Apparatus Details

The experimental setup consists of a computer, a computer screen, and an external haptic device. The experiments were conducted using the "Touch X" haptic device from 3D Systems, which boasts a 6-degrees-of-freedom (6DOF) positional sensing capability and 3-degrees-of-freedom force feedback. Notably, while the device can operate in 6DOF, we exclusively utilized its capability on the horizontal x-axis for this

study. Its nominal position resolution exceeds 1100 dpi (0.023 mm). The interface between the haptic device and the computer was facilitated using the OpenHaptics toolkit (version 3.5.0) from 3D Systems.

Haptic devices are commonly used alongside 3D graphics. While graphics require a refresh rate of 30-60 frames per second (fps) for continuous imagery, haptic feedback needs around 1000 fps due to the nuances of human perception. These different rates are often managed by running them in separate processes. To handle these varying rates, haptic and graphic updates run in separate processes. OpenHaptics toolkit, comprising the Haptic Device API (HDAPI) and QuickHaptics micro API, allowed direct force rendering. The servo loop rate of 1 kHz ensures that the system operates in real-time, allowing instantaneous feedback and seamless interactions. The graphics loop update is at a rate of 30 Hz. The entire experimental software was developed in C++ language, leveraging the capabilities of both HDAPI and QuickHaptics API for precise control and feedback. The Touch X device that we used can be seen in Fig. 2.1.

To use the haptic device user grips the pen-like stylus of the device, and the subject's one-dimensional (1D) motion is transferred to the simulation environment by taking the position, velocity, and acceleration information of the tip of the stylus.

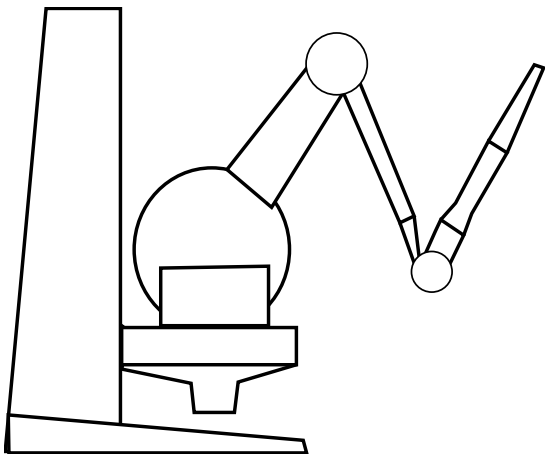

Figure 2.1: 3D Systems Touch X Haptic Device, side view

2.2 Experiments

In this section, we provide a comprehensive overview of our research methodology. We describe the experimental setup and the various scenarios designed to probe visual-motor integration abilities. We then outline the sequence in which these experiments were conducted, followed by details on the instructions given to participants, and our data collection methods.

2.2.1 Experimental Setup

Experiments were conducted during daytime hours to ensure participants' comfort and prevent eye strain, with low-level night lighting maintained throughout the sessions. The experimental setup was designed to minimize distractions. Participants faced a plain wall; the only other individual in the room was the researcher overseeing the experiment. The animation on the screen refreshed at a rate of 30 Hz. To eliminate unmodeled feedback, we positioned subjects so they could not visually observe their hands. The computer screen was set on a desk, approximately 50 cm away from the subjects, with the haptic device positioned beneath the desk. Subjects interacted with the device using its stylus. Refer to the illustration of the experimental setup in Fig. 2.2 for a better understanding.

Before starting each session, we calibrated the Touch X device using its diagnostic interface to ensure precise tracking and feedback.

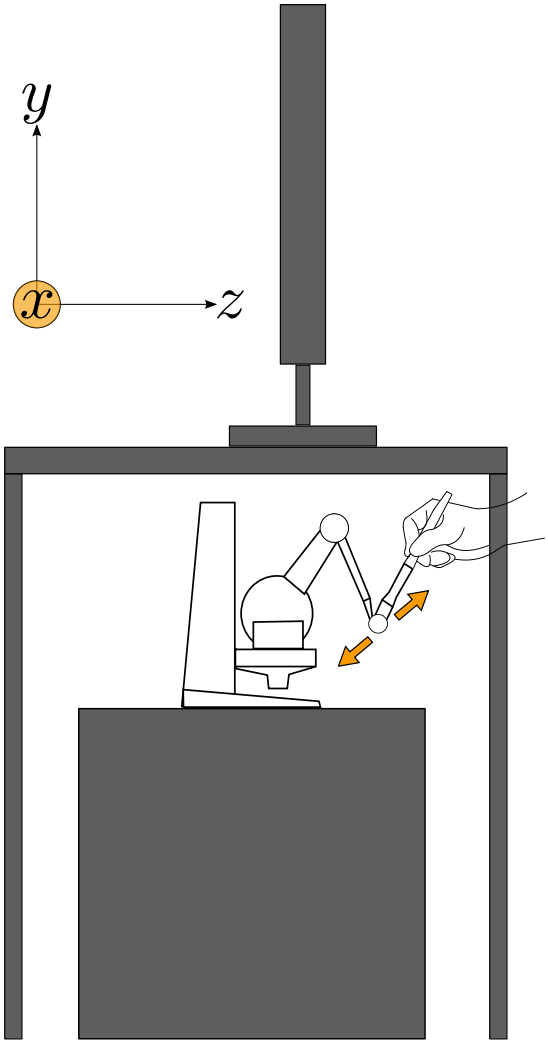

Figure 2.2: Illustration of the experimental setup, the positioning of the computer screen, and the haptic device.

2.2.2 Experimental Scenarios

Using a target-tracking task, we designed four experimental scenarios to examine various facets of the subjects' visual-motor integration abilities. We introduced two distinct trajectory types, single-frequency sinusoids and sum-of-sine, and operated on two different experimental scenes.

We can see the illustration of the first experimental scene on the left side of Fig. 2.3. Fig. 2.4 shows a screen capture of the implemented experimental scene on the left. In this scene, the operator can see the target and itself on the screen. The second

experimental scene is illustrated and captured on the right side of Fig. 2.3 and Fig. 2.4, respectively. The target and the operator are invisible. Instead, participants are given error information, represented by an error bar on the screen, indicating the difference between the target's and the subject's positions.

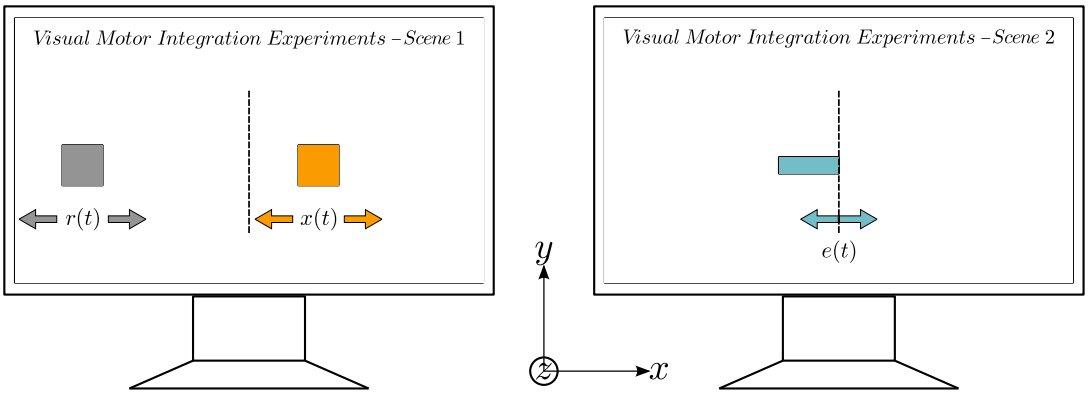

Figure 2.3: Illustration of experimental scenes: the first (left) and the second scene (right)

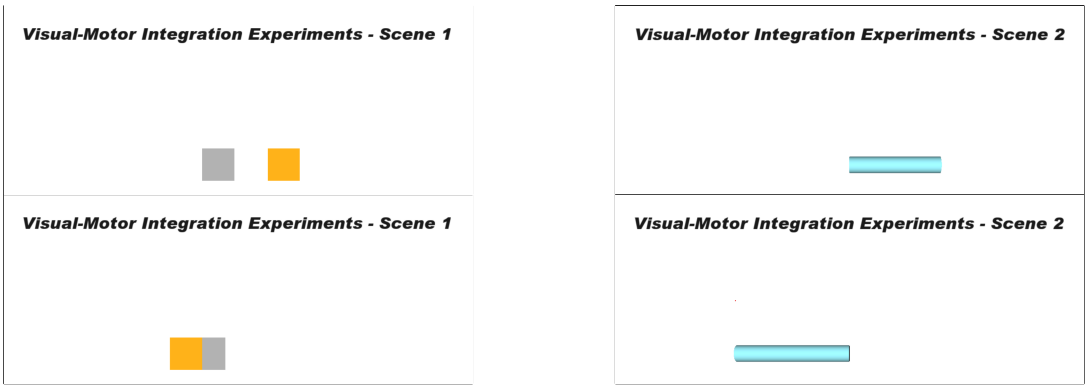

Figure 2.4: Screen capture of the implemented experimental scenes: the first (left) and the second scene (right). Upper and lower images show the horizontal movement on the screen.

On the left-hand side of Fig. 2.3, $x(t)$ denotes the subject's position, which translates to the center of the orange square on the screen, while $r(t)$ indicates the target object's position, taken from the gray square's center. On the right, $e(t)$ signifies the difference between the target and the subject's positions, such that $e(t) = y(t) - x(t)$. However, the actual positions, $x(t)$ and $r(t)$, are not shown to the subjects in this second scene.

In the first experimental scenario, namely Experiment 1, the first experimental scene is used. The operator can see the target and itself on the screen. The task is to track the target object animated on the computer screen using the haptic device as a medium. In this scenario, the target has a single-frequency sinusoidal trajectory described in (2.1). This scenario is repeated for five different frequencies, for $f_1 = 0.10$ Hz, $f_2 = 0.25$ Hz, $f_3 = 0.55$ Hz, $f_4 = 0.85$ Hz, and $f_5 = 1.0$ Hz. The amplitude of the trajectories is 20 mm. Movement velocity requirements vary between 0.2π cm/s to 2π cm/s.

$$r(t)_m^{SS} = 10sin(2pif_m t), \text{ for m = 1,2,..,5} \tag{2.1}$$

In the second experimental scenario, Experiment 2, participants track a sum-of-sine signal depicted in (2.2). This scenario uses the first experimental scene, similar to Experiment 1. The goal remains to follow the target object as closely as possible. To create a signal without any pattern, we introduced random phase differences ϕ^m to each sine component of the input.

$$r(t)^{SoS} = \sum_{m=1}^{5} = 5sin(2pif_m t + \phi_m) \tag{2.2}$$

The third experimental scenario, Experiment 3, requires subjects to track an input with a single-frequency sinusoidal trajectory for several frequencies, similar to Experiment 1. However, in this scenario, second experimental scene is used. The aim is to minimize the error bar animated on the screen as much as possible.

In the fourth and final experimental scenario, Experiment 4, tracking trajectory is a sum-of-sines signal, like Experiment 2. On the other hand, this scenario uses the second experimental scene like Experiment 3. The objective is to minimize the error bar animated on the screen.

In summary, Experiments 1 and 2 utilize the first experimental scene differing trajectory signals. Experiments 3 and 4 use the second experimental scene with the difference created again by the introduced input.

Details of the four main groups of experiments are given below.

1. Experiment 1: Single Frequency Sinusoidal Signal Tracking:

    - Subjects were tasked with tracking a target, represented as a box on the screen, moving in a single-frequency sinusoidal trajectory along the horizontal axis.
    - Boxes with identical dimensions visually represent the target and the operator.
    - We repeated this experiment for several single-frequency sinusoids with frequencies of 0.1 Hz, 0.25 Hz, 0.55 Hz, 0.85 Hz, and 1 Hz. The trajectory maintained a consistent amplitude of 2 cm, resulting in varying target velocities, with 1 Hz being the most rapid.

2. Experiment 2: Sum-of-Sines Signal Tracking:

    - Similar to Experiment 1, subjects were tasked with tracking a target, represented as a box on the screen, moving in a sum-of-sines trajectory along the horizontal axis.
    - Boxes with identical dimensions visually represent the target and the operator.
    - EEach sinusoidal component of the sum-of-sine signal has the same amplitude, and incorporated phase differences introduce unpredictability. See Eq. (2.2) for details.

3. Experiment 3: Error Minimization with Single Frequency:

    - Unlike the previous scenarios, the target and operator are not visible—instead, the error signal representing the difference between the target and the subject's position is given.
    - The objective was to minimize this error, represented by a bar on the screen.
    - The target followed several single-frequency sinusoidal trajectories with the frequencies mentioned earlier. The amplitude remained fixed at $20mm$.

4. Experiment 4: Error Minimization with Sum-of-Sines:

    - Similar to the third scenario, only the error signal is present.

- The target's movement was defined by a sum-of-sine signal, with each component having the same amplitude and a phase difference to introduce unpredictability. See Eq. (2.2) for details.

All experimental tasks necessitate unidirectional movement, specifically along the horizontal axis (left to right), using either the wrist or the arm. Participants received solely visual feedback during the experiments.

2.2.3 Experimental Sequence

The experiments followed a specific sequence to ensure consistency and accuracy. Initially, the single-frequency sinusoidal trajectory experiments (Experiment 1 & Experiment 3) were conducted in a randomized frequency order for each participant, meaning each subject experienced the experiments in a unique sequence. Every frequency was tested twice in one-minute sessions. Subjects first undertook Experiment 1, followed by Experiment 3 for the same frequency. After completing Experiment 1 and 3, the sum-of-sines experiments (Experiment 2 & Experiment 4) were carried out four times in one-minute sessions. An example of the entire experimental sequence is illustrated in Table 2.1.

Table 2.1: A randomized experimental sequence example.

Step	Experiment Number	Length (sec)	Trial
Step 1	Exp. 1 f_2	60	2
Step 2	Exp. 3 f_2	60	2
Step 3	Exp. 1 f_4	60	2
Step 4	Exp. 3 f_4	60	2
Step 5	Exp. 1 f_3	60	2
Step 6	Exp. 3 f_3	60	2
Step 7	Exp. 1 f_5	60	2
Step 8	Exp. 3 f_5	60	2
Step 9	Exp. 1 f_1	60	2
Step 10	Exp. 3 f_1	60	2
Step 11	Exp. 2	60	2
Step 12	Exp. 4	60	2
Step 13	Exp. 2	60	2
Step 14	Exp. 4	60	2

We gave 30-45 seconds rest periods between each step to subjects. Combined with the rest periods (from Step 1 to the end of Step 10), Experiment 1 and Experiment 3 took approximately 30 minutes, while Experiment 2 and Experiment 4 lasted around 14-15 minutes. The entire experimental procedure, from initiation to finish, spanned about 45 minutes. When factoring in the training period, the total duration for each participant reached approximately one hour.

2.2.4 Instructions to Participants

Participants received a briefing about the experimental procedure, which included details about their seating arrangement, designed to obscure their hand movements, and guidance on the proper use of the haptic device. To prevent potential bias, we did not disclose the overarching objectives of the study, such as the nature of the

upcoming input or strategies for successful task completion. For Experiments 1 and 2, participants were told that their movements would be represented by an "orange" square on the screen, which they should aim to align with a "gray" target square. In Experiments 3 and 4, subjects were instructed to minimize the width of a displayed "blue" error bar.

A training session was conducted after this orientation, allowing participants to familiarize themselves with the tasks. This session allowed them to practice each experiment they would later perform in the main experimental phase. Each training task lasted approximately 45 seconds. After the training, participants were given a 15-minute rest before initiating the primary experiments.

2.2.5 Data Collection

Data was captured at an almost flawless rate of 1 kHz, capturing the target's position, the participant's position, and the participant's velocity. Positional data was measured in millimeters, while velocity data was recorded in millimeters per second. Only the central 40 seconds of the one-minute data set was used for analysis purposes. We excluded each experiment's initial and final 10 seconds to account for potential biases, such as diminishing attention or fatigue.

CHAPTER 3

TASK PERFORMANCE AND ANALYSIS METHODS

In this chapter, we introduce the performance metrics we used to measure the success of the participants' tracking behavior. We also discuss why some participants are not included in the analysis. In addition, we describe in detail the analysis techniques we used to examine our data.

Table 3.1 represents the parameters used in this chapter and their meanings.

Table 3.1: Parameters and their definitions

Parameters	Description	Units
Discrete-time variables		
t_a	Analyzed experiment length	sec
F_s	Servo loop sampling rate	Hz
f_m	Single sine input frequency	Hz
x_i	Subject position at i^{th} step	mm
r_i	Target position at i^{th} step	mm
e_i	Position error at i^{th} step	mm
Frequency Domain Terms		
$X(j\omega)$	FFT of x_i signal	
$R(j\omega)$	FFT of r_i signal	
$T(j\omega)$	FFT of the transfer function	

3.1 Task Performance

In our study, we conducted 1D manual target-tracking experiments in a virtual reality environment with 25 participants. We conducted four tracking task scenarios with each subject and recorded their activity. It was imperative to establish a robust performance metric to evaluate the proficiency of each participant's performance and exclude the participants with insufficient performance to achieve a meaningful outcome from the response.

3.1.1 Mean Squared Error

We chose the Mean Squared Error (MSE) as our primary evaluation criterion for the subject's task success. Mathematically, MSE is defined as:

$$MSE = \frac{1}{n}\sum_{i=1}^{n}(r_i - x_i)^2 = \frac{1}{n}\sum_{i=1}^{n} e_i^2 \tag{3.1}$$

Here, n is the total number of time steps of the analyzed fragment of the data. In our case, it is $F_s.t_a = 40000$.

MSE quantifies the average deviation between the target's path and the participant's tracking movement. A lower MSE value indicates that the participant closely followed the target's trajectory, reflecting a higher tracking accuracy. Conversely, a larger MSE suggests potential deviations from the target's path, indicating less precise tracking.

Given the nature of our experiment, the MSE is especially relevant. It provides an average measure of tracking accuracy and emphasizes more significant deviations, ensuring that participants' tracking remains consistently close to the target throughout the experiment. Based on the mean MSE values of all participants, we established a threshold to determine the participants' success for each experiment. Participants with an MSE exceeding this threshold were deemed to have insufficient tracking accuracy and were subsequently excluded from the final results. This approach ensured that our results were derived from participants who accurately demonstrated a consis-

tent tracking performance. We ensured that if the subjects exceeded the threshold of any experiment, they would be exempted from all of the experiments.

We determined the threshold based on the 95^{th} percentile, which refers to the value below which 95% of the MSE falls. In other words, only 5% of the MSE is above this value. This term can be represented as:

$$P(MSE \leq P) = 0.95 \tag{3.2}$$

For Experiment 1 and Experiment 3, mean value of the MSE is calculated as:

$$mean_{m=1}^{5}\, mean_m(\text{first trial mse}(f_m)\&\text{second trial mse}(f_m)) \tag{3.3}$$

It means that we first take the mean of two trials for each frequency. Then, the mean MSE is calculated by taking the mean of every single sine experiment for each individual. For Experiment 2 and Experiment 3, the mean MSE is calculated by averaging the MSE values of each trial.

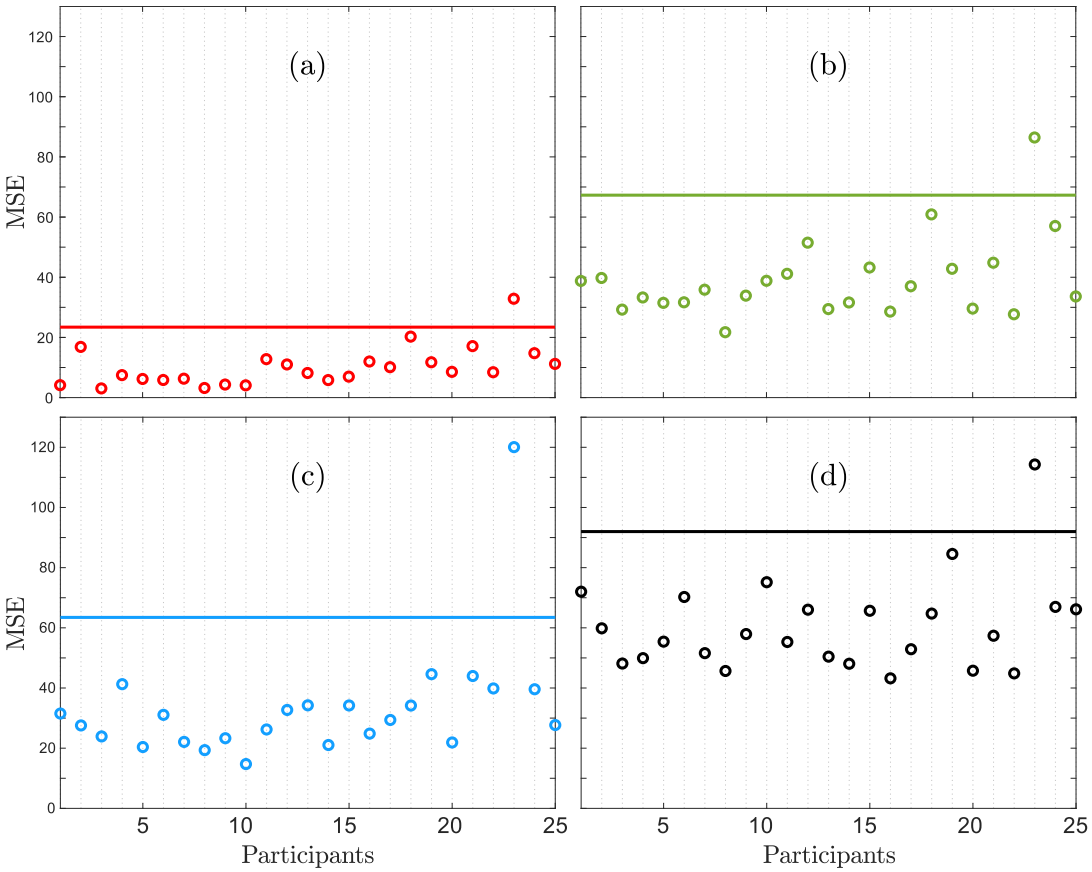

Figure 3.1: Mean MSE distributions for all experiments and all participants: (a)Experiment 1, (b) Experiment 2, (c) Experiment 3, (d) Experiment 4. The solid line represents the 95th percentile of each experiment's mean MSE, respectively. Circles are the mean MSE of each participant individually.

As seen in Fig. 3.1, the 23^{rd} subject could not perform successfully and has a mean MSE above the threshold for all experiments. This subject is exempted from the analysis.

3.2 System Identification

System identification is used to construct mathematical models of dynamic systems based on observed data. In our experiment, where human subjects are tasked with tracking a target in a virtual reality environment, system identification allows us to understand the dynamic relationship between the target's movement (input) and the

subject's response (output). This understanding is crucial for quantifying the subject's tracking ability and predicting their response to different target trajectories.

3.2.1 Non-Parametric Transfer Function Extraction

One approach to system identification is the non-parametric method, which does not assume any specific model structure but instead derives the system's response directly from the data. Our study focused on the non-parametric transfer function, which provides a frequency domain representation of the system's dynamics.

We have five distinct single-frequency sinusoidal trajectories for the target in Experiment 1 and 3. We recorded the tracking response of subjects for each trajectory. Using the Fast Fourier Transform (FFT), we extracted the frequency components of both the target's trajectory and the subject's response. The transfer function, the ratio of the subject's output to the target's input in the frequency domain, was computed for each frequency. Combining the results from all five trajectories, we constructed a Bode plot, which graphically represents the magnitude and phase of the transfer function across the frequency spectrum.

Mathematically, for a given frequency $2\pi f_m = \omega_m$:

$$T(j\omega) = \frac{X(j\omega)}{R(j\omega)}, \text{ at frequencies } \omega_1, \omega_2, .., \omega_5 \tag{3.4}$$

In Experiment 2 and 4, we introduce a more complex trajectory for the target, a sum-of-sine signal with each sinusoidal signal having distinct phase differences to avoid introducing a predictable pattern. As with the single sine trajectories, we recorded the subject's response and used FFT to extract the frequency components. The Bode plot response was then derived using the same approach as before. The advantage of using a sum-of-sine signal trajectory is that it allows for simultaneous testing of the system's response at multiple frequencies, providing a comprehensive view of the system's dynamics.

It is important to note that our analysis operates under the assumption of linearity, which means that we assume the relationship between the target's movement and

the subject's response is linear, and superposition applies. While this simplifies our analysis and the resulting models, potential nonlinearities in the subject's response could be considered in future studies.

While presenting our findings, we use the mean response of the participant group. However, this method tends to overlook the inherent variability among individuals. To address this limitation, we also establish a confidence region around the derived magnitude and phase responses. To bound our results, we determine the lower and upper limits by calculating the lower quartile (25^{th} percentile) and the upper quartile (75^{th} percentile), calculated as given in Eq. (3.5) and Eq. (3.6), respectively.

$$P(MSE \leq P_{lower}) = 0.25 \tag{3.5}$$

$$P(MSE \leq P_{upper}) = 0.75 \tag{3.6}$$

We also present our phase and magnitude responses on a complex plane. Complex plane characterization can be denoted as:

$$\alpha e^{i\theta} \tag{3.7}$$

Furthermore, it can represent the response at a distinct frequency. Here, α is the magnitude calculated as:

$$\alpha = |T(jw_m)| \tag{3.8}$$

Here θ shows the phase lag and computed as

$$\theta = \frac{imaginary(T(jw_m))}{real(T(jw_m))} \tag{3.9}$$

In this characterization, we use the unit circle as a reference point to symbolize the perfect response of one. On the other hand, the positive real axis represents perfect tracking with zero lag.

3.2.2 Noise Content Characterization

As we change the experimental scene, we introduce unpredictability to the experiments. Noise content characterization is a process used to understand the nature and presence of unwanted or extraneous signals within recorded data. In both Experiment 2 and Experiment 4, we track a sum-of-sine signal. By taking the FFT of the output, one can identify the specific frequency components of the signal. To exclusively analyze the noise, the frequencies corresponding to the stimulus are removed. What is left, representing the noise, is then compared, helping us measure the noise content in our experiments.

CHAPTER 4

RESULTS AND DISCUSSION

In this chapter, we delve into the outcomes of our experiments, presenting the data we have gathered. We will explore the results, offering interpretations and discussing their significance in the context of visual-motor integration abilities. Through a balanced analysis, we aim to provide a clear understanding of what our findings suggest and their implications for the broader field.

4.1 Results

In Experiment 1, we recreated the human pursuit control task. The Bode plot depicted in Fig. 4.1 provides valuable insights into human motor control and response when the input is predictable and direct visual feedback from the target's and subject's position is available. The magnitude and phase response of the bode plot show a slight decline as frequency increases, suggesting that participants found it more challenging to track the target at higher frequencies. This behavior is consistent with the nature of human motor response, where rapid movements can be more challenging to execute with precision. Also, this result is consistent with the outcome presented in [39].

The confidence region's variability across frequencies further elucidates this observation. A narrow confidence region at 0.1 Hz indicates consistent tracking by participants at lower frequencies, benefiting from the slower target movement and ample time to adjust based on visual feedback. However, the wider confidence region at 1 Hz reveals increased response variability, likely due to the combined effects of neural processing delays, muscle response times, and the inherent challenges of rapid target tracking. While aiding in the tracking task, the direct visual feedback might have

become more challenging for participants to process in real time as the frequency increased, leading to the observed variability in response. Overall, the results underscore the complexities and limitations of human motor control, mainly when tasked with tracking rapid movements.

Then again, as seen from the complex plane representation of the mean response given in Fig. 4.2, the response is distributed in a small spectrum and does not vary much. Subjects possess a consistent, near-perfect performance.

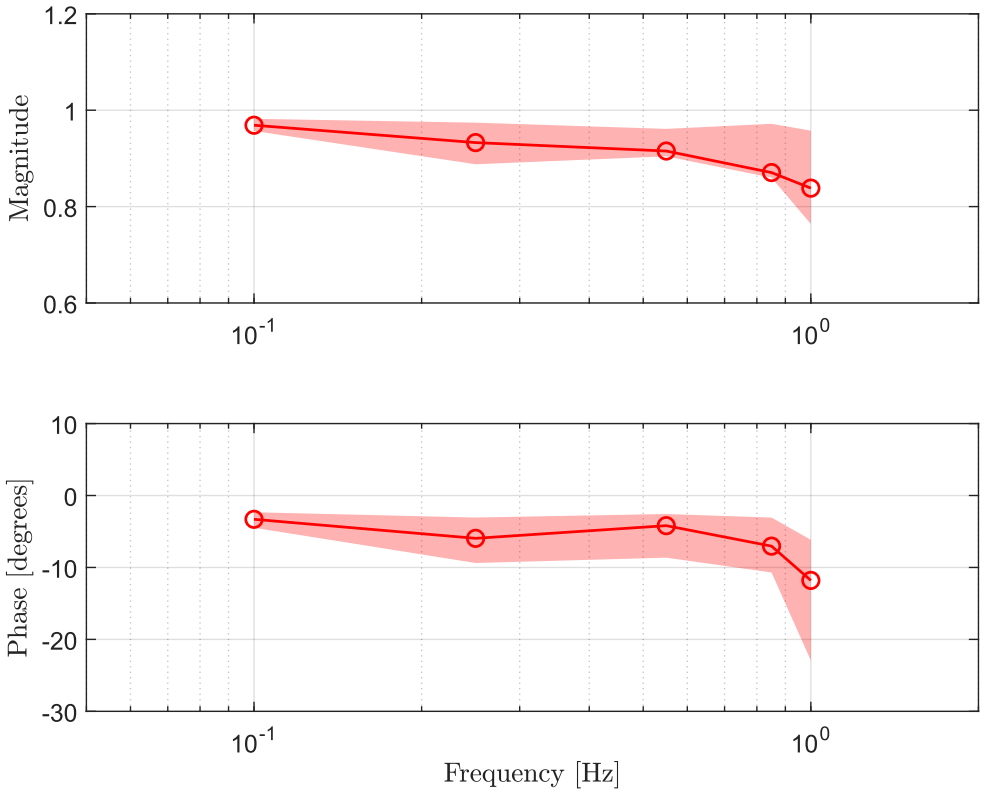

Figure 4.1: Experiment 1 magnitude and phase response plot. The solid lines represent the mean response, while the transparent bounds correspond to the confidence region calculated between the first and last quartile.

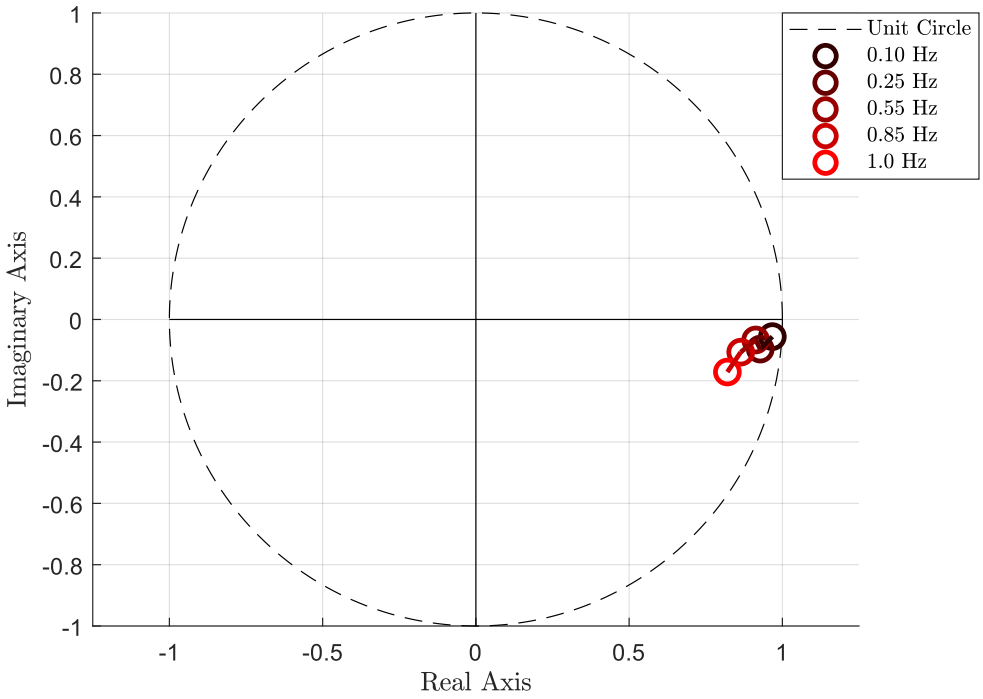

Figure 4.2: Experiment 1 response on complex plane. Each circle corresponds to the response at stimulus frequencies, the darkest shade for the smallest frequency and the lightest shade for the largest frequency component of the experiment. The unit circle symbolizes the perfect tracking with gain one as a reference point, and the positive real axis represents the perfect phase with zero lag.

In Experiment 2, we created a variation of the pursuit control task with a sum-of-sines signal trajectory, with direct visual feedback of both the target's and subject's positions. The Bode plot given in Fig. 4.3 reveals distinct characteristics of pursuit control display under more complex input signals. The magnitude response decreases as the frequency increases, starting from 0.675 at 0.1 Hz and dropping to 0.413 at 0.25 Hz. However, at 1.0 Hz, there is a noticeable upward trend in magnitude response, rising up to 0.927. The magnitude response for Experiment 2 started high, went lower for middle frequencies, and then rose again for the highest frequency, forming a 'U' shape. This "U" shape suggests that while participants might find tracking the target at intermediate frequencies challenging, they seem to adapt better at the highest frequency tested.

The phase response shows a consistent lag across all frequencies, with the phase de-

lay increasing from -31.1° at 0.1 Hz to -46.6° at 1 Hz, indicating that participants consistently lagged behind the target's movement, with the lag becoming more pronounced at higher frequencies.

The confidence regions provide additional insights into the consistency of participants' responses. The magnitude confidence region is narrowest at 0.1 Hz, indicating consistent tracking at this frequency. However, the confidence region widens as the frequency increases, suggesting more variability in participants' tracking ability. This widening is particularly apparent at 0.25 Hz and 0.55 Hz, where the upper and lower bounds of the magnitude show significant differences. The phase confidence region also shows increased variability at higher frequencies, reinforcing the notion of increased challenges in tracking rapid and complex movements.

The complex plane representation of the response given in Fig. 4.4 suggests similar outcomes. The response lags the input and gets worse as the frequency increases. Nevertheless, the response at 1 Hz deserves special consideration since it contradicts the intuition. We will further discuss this phenomenon in the upcoming sections.

Experiment 2 highlights the intricacies of human pursuit control tasks when faced with unpredictable input signals. While participants can track slower and simpler movements with relative consistency, the challenges of tracking rapid and compound movements become evident, as reflected by the decreasing magnitude response and increasing phase lag.

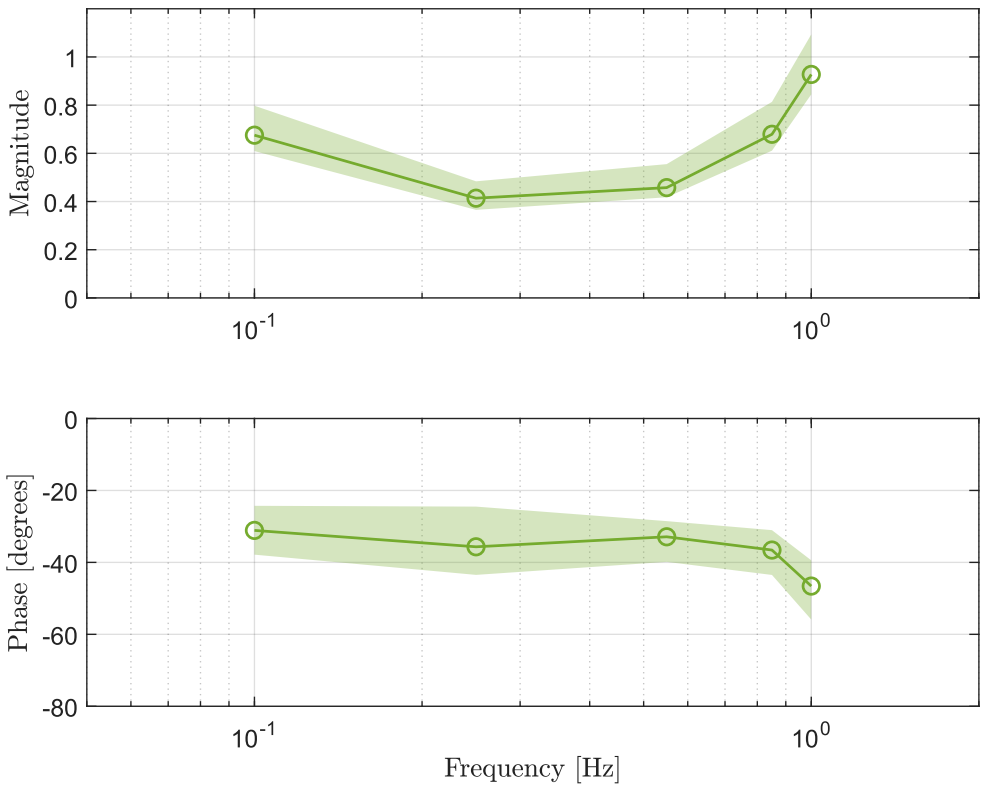

Figure 4.3: Experiment 2 magnitude and phase response plot. The solid lines represent the mean response, while the transparent bounds correspond to the confidence region calculated between the first and last quartile.

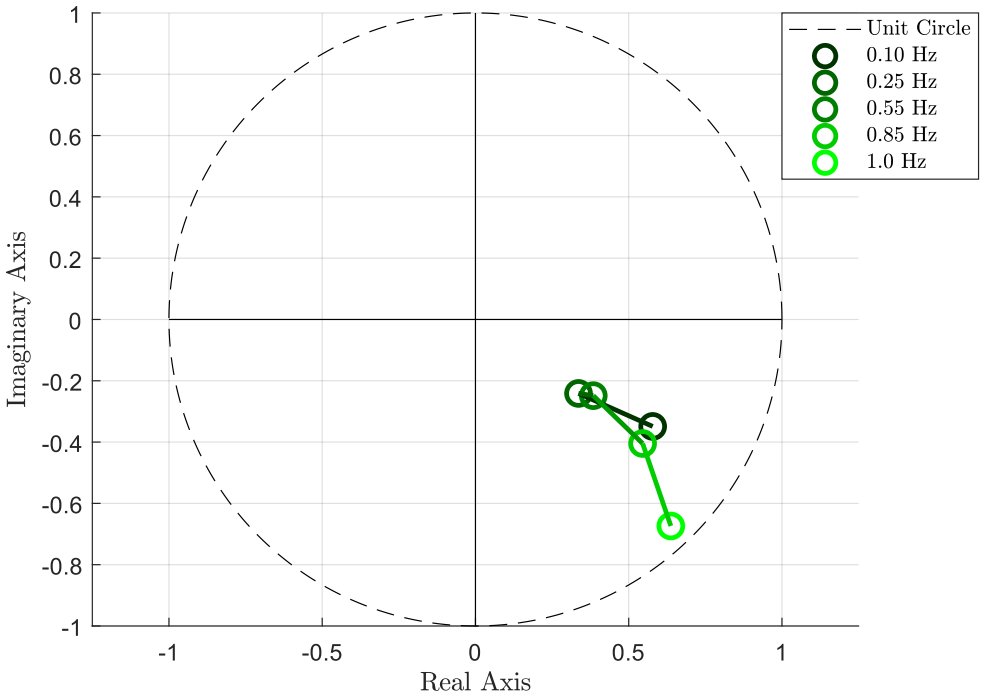

Figure 4.4: Experiment 2 response on complex plane. Each circle corresponds to the response at stimulus frequencies, the darkest shade for the smallest frequency and the lightest shade for the largest frequency component of the experiment. The unit circle symbolizes the perfect tracking with gain one as a reference point, and the positive real axis represents the perfect phase with zero lag.

In Experiment 3, we created a task to track several single-frequency sinusoidal signals without direct visual feedback of the target's or subject's positions. This experiment is a variation of the compensatory control task presented in [31], yet different from the original version; input is predictable. We only provided error signals to subjects, and the task was to minimize this error shown by a bar as much as possible. The Bode plot for this experiment depicted in Fig. 4.5 offers insights into how humans adapt to such conditions.

The magnitude response starts strong at 0.993 for 0.1 Hz, indicating near-perfect tracking at this frequency. However, as the frequency increases, the magnitude response drops significantly, reaching as low as 0.281 at 1.0 Hz. This decline suggests that participants found it increasingly challenging to track the target accurately as the frequency increased, especially without direct visual feedback of positions.

The phase response shows a consistent lag across the tested frequencies, starting from -9.67° at 0.1 Hz and increasing to -32.6° at 1.0 Hz. This phase lag indicates that participants were consistently behind the target's movement, with the delay becoming more pronounced as the frequency increased.

At 0.1 Hz, the magnitude confidence region is relatively narrow, suggesting consistent tracking by most participants. However, the confidence region widens as the frequency increases, especially at higher frequencies like 0.85 and 1.0 Hz. This widening indicates increased variability in participants' tracking abilities under these conditions. The phase confidence region also shows increased variability, particularly at frequencies like 0.55 and 0.85 Hz.

The complex plane representation of the response in Fig. 4.6 suggests a consistent response drop as the frequency increases.

In summary, Experiment 3 underscores the challenges faced by participants when deprived of direct visual feedback of positions. While they could track slower movements with relative accuracy, the complexities of tracking rapid movements without direct positional feedback became evident. The decreasing magnitude response and increasing phase lag, coupled with the widening confidence regions, highlight the limitations of human compensatory tracking control under such conditions.

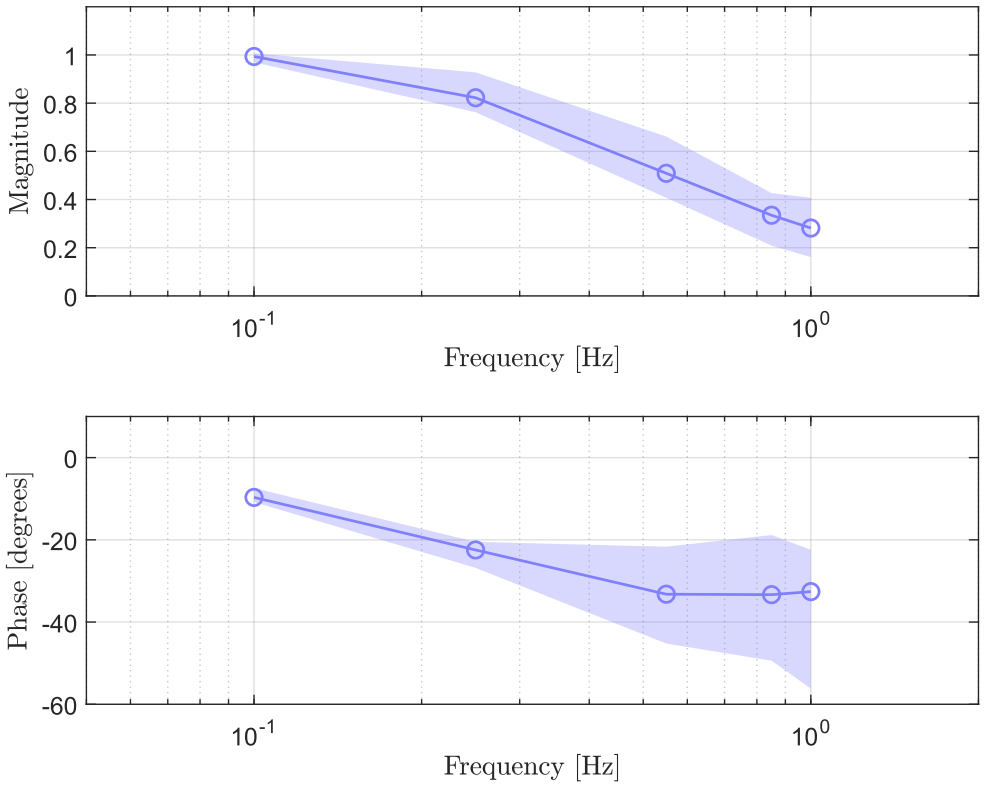

Figure 4.5: Experiment 3 magnitude and phase response plot. The solid lines represent the mean response, while the transparent bounds correspond to the confidence region calculated between the first and last quartile.

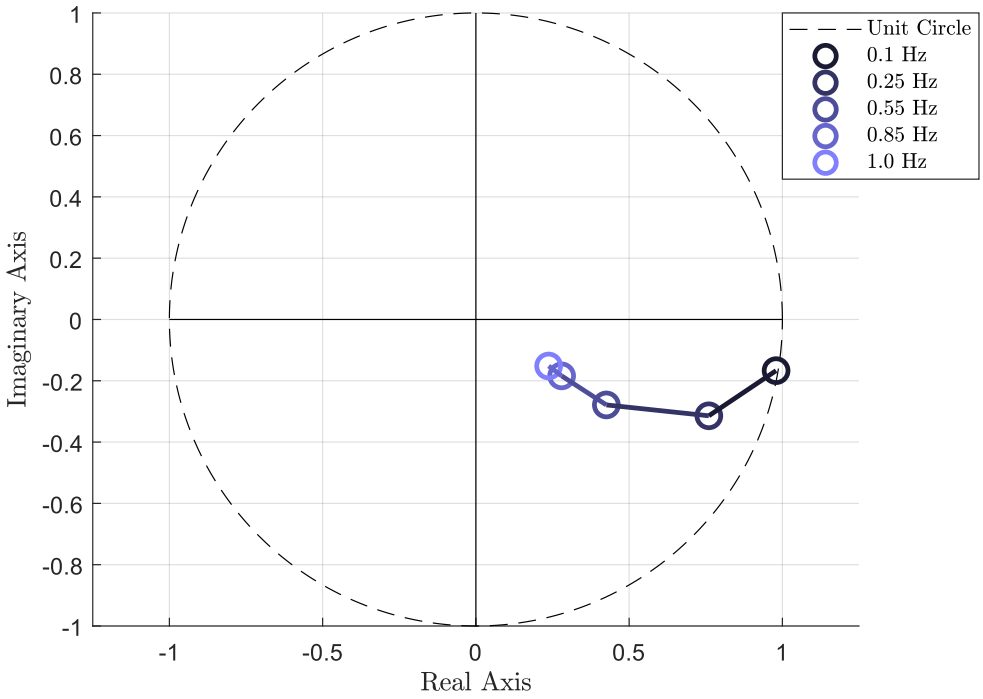

Figure 4.6: Experiment 3 response on complex plane. Each circle corresponds to the response at stimulus frequencies, the darkest shade for the smallest frequency and the lightest shade for the largest frequency component of the experiment. The unit circle symbolizes the perfect tracking with gain one as a reference point, and the positive real axis represents the perfect phase with zero lag.

Experiment 4 creates the most complex scenario for tracking. The task is to minimize the errors without direct visual feedback of the target's or subject's positions when the input is an unpredictable sum-of-sines signal. This experiment creates a complete replica of the compensatory control task. In this experiment, both the input and the scene introduce unpredictability to the tracking task. The Bode plot given in Fig. 4.7 for this experiment reveals the intricacies of human motor control under these conditions.

The magnitude response starts at 0.465 for 0.1 Hz, indicating that participants could moderately track this frequency component of the input sum-of-sines signal. However, as the frequency increases, the magnitude response dips, reaching a minimum of 0.197 at 0.55 Hz before slightly increasing again. Like Experiment 2, the magnitude response for Experiment 4 started high, went lower for middle frequencies, and then

rose again for the highest tested frequency, forming a 'U' shape. This pattern suggests that participants found it most challenging to track the target around the mid-range frequencies.

The phase response consistently lags across the tested frequencies, starting from $-50.95\circ$ at 0.1 Hz and increasing to $-66.1\circ$ at 1.0 Hz. This consistent phase lag indicates that participants were always behind the target's movement, with the delay becoming more pronounced as the frequency increased.

The confidence regions provide insights into the variability in participants' responses. At 0.1 Hz, the magnitude confidence region is relatively broad, suggesting varied tracking capabilities among participants. This variability becomes even more pronounced at higher frequencies, such as 0.85 and 1.0 Hz. The phase confidence region also shows increased variability across all frequencies, indicating that participants' reactions to the sum-of-sines signal were diverse.

From the complex plane representation given in Fig. 4.8, we see that the response is almost like a noise response, and the subjects were almost unable to follow the input at most frequencies. Again, like Experiment 2, the response at 1 Hz deserves special consideration since it contradicts the intuition, and we will further discuss this phenomenon in the upcoming sections.

Experiment 4 highlights human compensatory control's complexities when tracking a sum-of-sine signal without direct positional feedback. The fluctuating magnitude response, increasing phase lag, and wide confidence regions emphasize the challenges participants faced under these conditions.

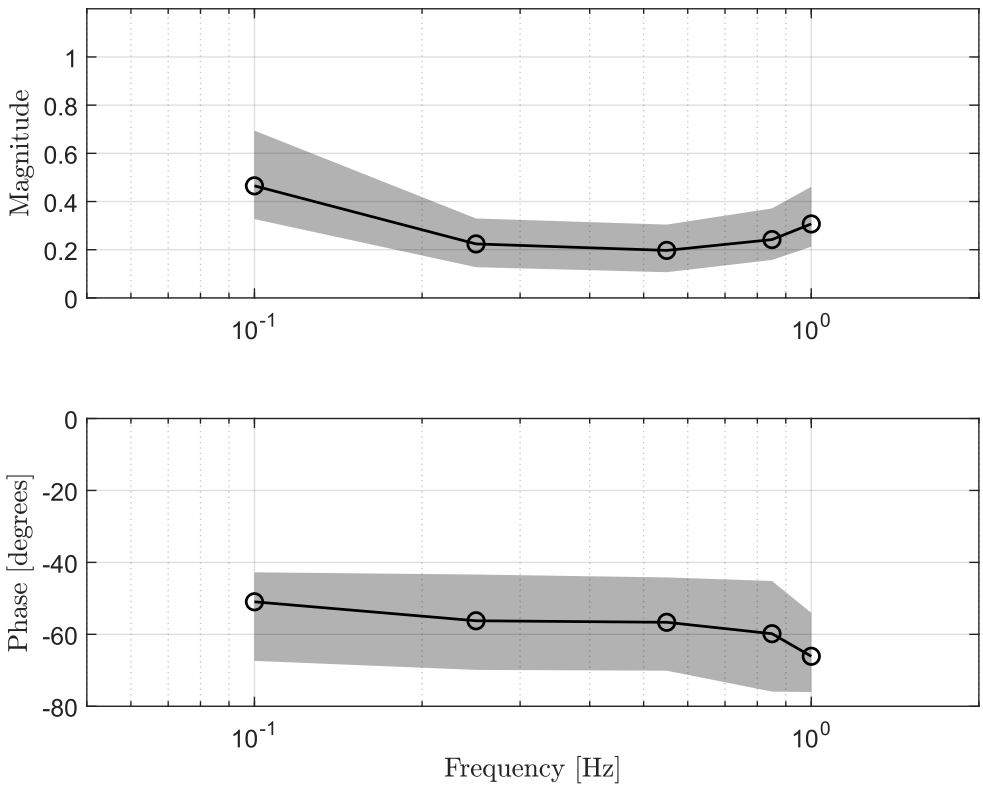

Figure 4.7: Experiment 4 magnitude and phase response plot. The solid lines represent the mean response, while the transparent bounds correspond to the confidence region calculated between the first and last quartile.

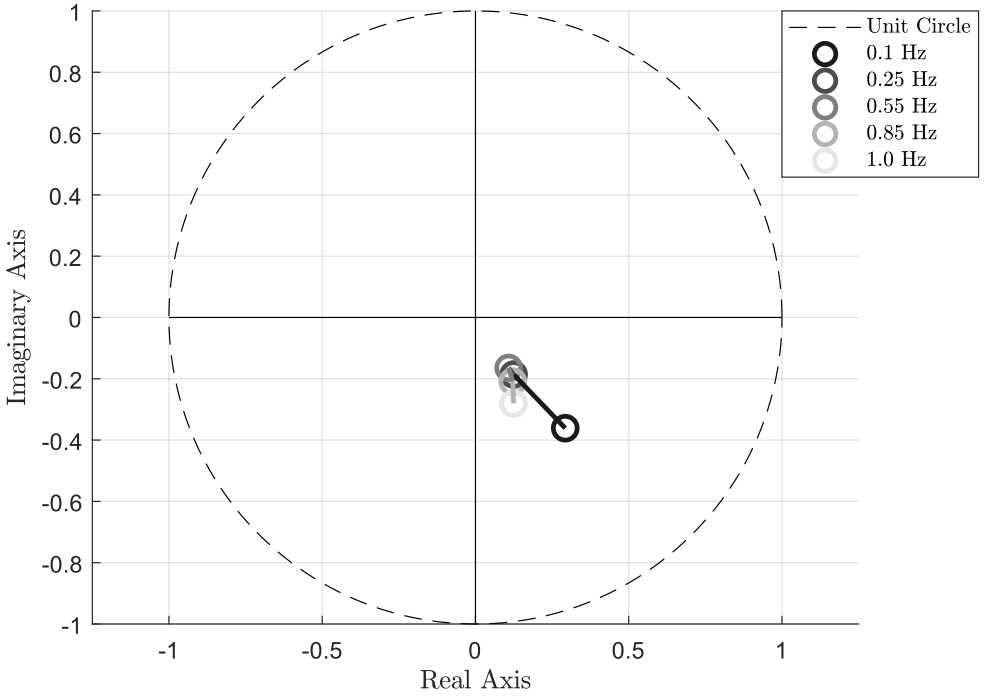

Figure 4.8: Experiment 4 mean response characterized by a point on the complex plane. Each circle corresponds to the response at stimulus frequencies, the darkest shade for the smallest frequency and the lightest shade for the largest frequency component of the experiment. The unit circle symbolizes the perfect tracking with gain one as a reference point, and the positive real axis represents the perfect phase with zero lag.

4.2 Comparison Between Experiment 1 and Experiment 2 (Predictable vs. Unpredictable Input With Direct Visual Feedback)

Both Experiment 1 and Experiment 2 shared the same experimental scene, creating variations of the pursuit control task. We provided direct visual feedback of both the target's and the subject's positions to participants. The primary distinction between the two was the nature of the tracking signal: a single sine wave in Experiment 1 versus a sum-of-sines in Experiment 2, where the sum-of-sines input decreased the predictability of the task.

In Experiment 1, participants displayed a relatively high magnitude response across the tested frequencies, which suggests that participants could track the single sine

wave with a high degree of accuracy, especially at lower frequencies. The phase response showed a gradual increase in lag, indicating a consistent but minor delay in participants' tracking relative to the target's movement. Contrastingly, in Experiment 2, the magnitude response was notably lower, which suggests that participants found it more challenging to track the sum-of-sines signal, especially at mid-range frequencies. The phase lag in Experiment 2 was also more pronounced than Experiment 1. This indicates a more significant delay in participants' reactions when tracking a more complex, unpredictable signal. The confidence regions for both experiments further emphasize the increased challenge of Experiment 2. While the confidence regions in Experiment 1 were relatively narrow, indicating consistent performance among participants, the regions in Experiment 2 were wider, especially at higher frequencies. This suggests more significant variability in participants' ability to track the sum-of-sines signal.

The human sensory-motor system is a dynamic control system that responds to external stimuli. In Experiment 1, where the input is a single-frequency sine wave, the system is subjected to a predictable and periodic stimulus analogous to a system tested with a simple harmonic input. Given the system's inherent design and prior experiences, it can effectively "tune" itself to this frequency, resulting in a more accurate and phase-aligned response. This is evident from the higher magnitude response, and more negligible phase lag observed in Experiment 1. Experiment 2 introduces a sum-of-sines signal, representing a superposition of multiple harmonic inputs. When faced with such a complicated input, a typical control system might find it challenging to track each frequency component accurately. This complexity is mirrored in the overall reduced magnitude response and increased phase lag of Experiment 2. The system's response becomes more reactive than predictive as it adapts to the rapidly changing input in real-time.

Biologically, the difference between the responses can be interpreted as the human brain's ability to anticipate and adapt to predictable patterns. The outcome might suggest that the neural pathways involved in sensory-motor integration become more efficient when exposed to a consistent stimulus, leading to improved tracking performance, and the unpredictability of the sum-of-sines input might be challenging the brain's anticipatory mechanisms. The wider confidence regions observed might be

attributed to the variability in individual neural responses to this unpredictable stimulus. Overall, this results in a better performance when the input has a recognizable pattern compared to a complex, unpredictable input.

In essence, comparing Experiments 1 and 2 provides a comprehensive understanding of how dynamic systems with perfect feedback react to different inputs. While the system can adeptly track simple, predictable inputs, its performance can fade when confronted with complicated and unpredictable stimuli, highlighting the significance of system adaptability and tuning in biological systems and control engineering.

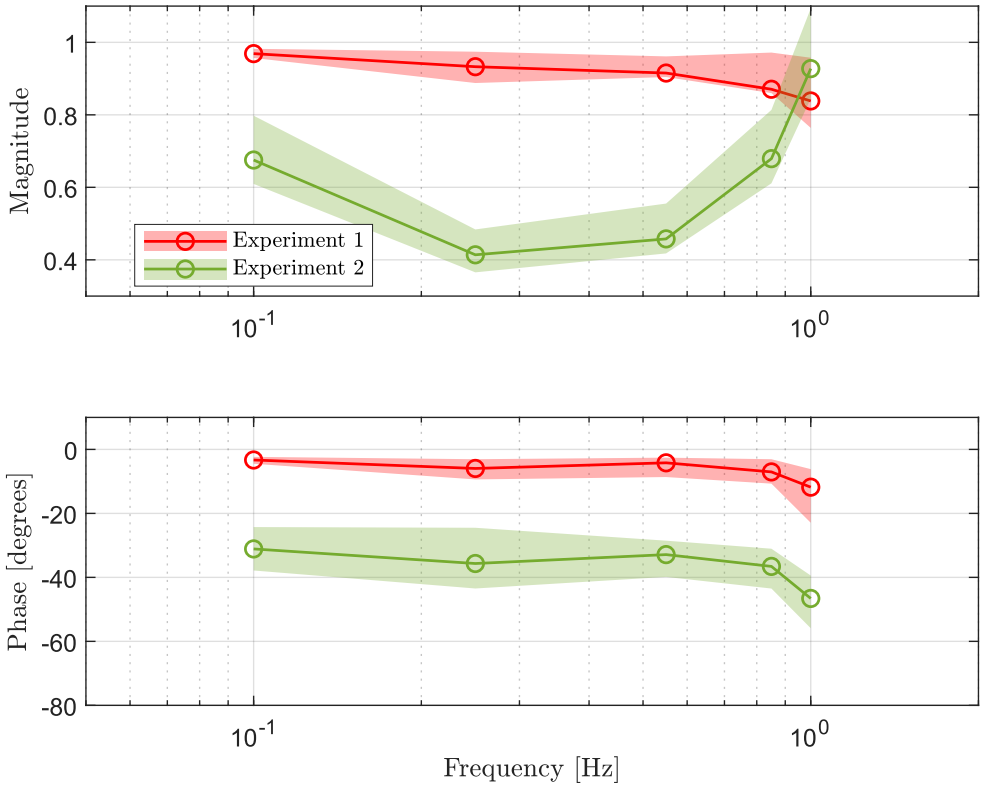

Figure 4.9: Comparison of magnitude and phase responses between Experiment 1 and Experiment 2, tracking of predictable input (red) versus unpredictable input (green) with direct visual feedback. The solid lines represent the mean response, while the same colored transparent bounds correspond to the confidence region calculated between the first and last quartile for respective experiments.

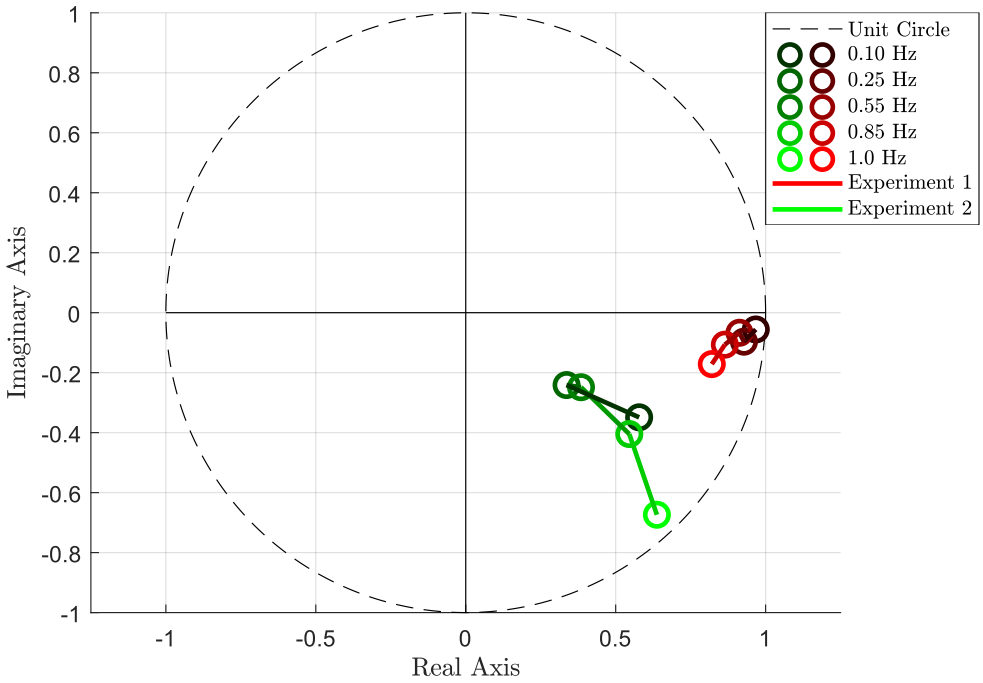

Figure 4.10: Comparison of system responses on a complex plane between Experiment 1 and Experiment 2, tracking of predictable input (shades of red) versus unpredictable input (shades of green)with direct visual feedback. Each circle corresponds to the response at stimulus frequencies, the darkest shade for the smallest frequency and the lightest shade for the largest frequency component of the experiments. The unit circle symbolizes the perfect tracking with gain one as a reference point, and the positive real axis represents the perfect phase with zero lag.

4.3 Comparison Between Experiment 1 and Experiment 3 (Predictable Input With vs. Without Direct Visual Feedback)

In comparing Experiment 1 and Experiment 3, the difference lies in the nature of the visual feedback provided to the subjects. Both experiments utilize the same single sine input signals, but the feedback mechanisms differ, leading to distinct behavioral and performance outcomes.

We observe distinct differences in magnitude and phase responses when examining the Bode plots of Experiment 1 and 3 in Fig. 4.11. For Experiment 1, the magnitude response remains relatively high across the tested frequencies, indicating a robust

tracking ability when direct visual feedback is provided. While showing a gradual lag, the phase response remains within a manageable range, suggesting that participants can effectively compensate for the phase differences introduced by the system dynamics. In contrast, Experiment 3 exhibits a more attenuated magnitude response, especially at higher frequencies, suggesting that the absence of direct feedback affects the participants' ability to track the target accurately, particularly at higher frequencies. The phase response for Experiment 3 also indicates a more pronounced lag, which we can attribute to the increased reliance on error feedback and the inherent challenges in processing this abstract form of feedback.

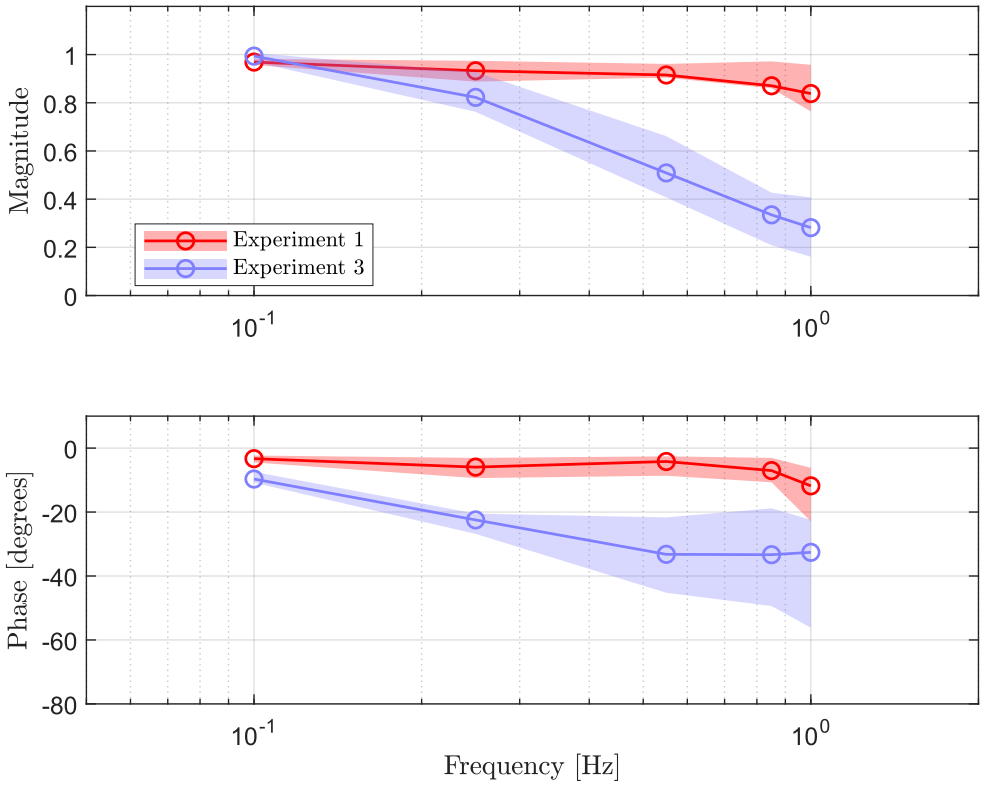

Figure 4.11: Comparison of magnitude and phase responses between Experiment 1 and Experiment 3, tracking of predictable input with (red) versus without (blue) direct visual feedback. The solid lines represent the mean response, while the same colored transparent bounds correspond to the confidence region calculated between the first and last quartile for respective experiments.

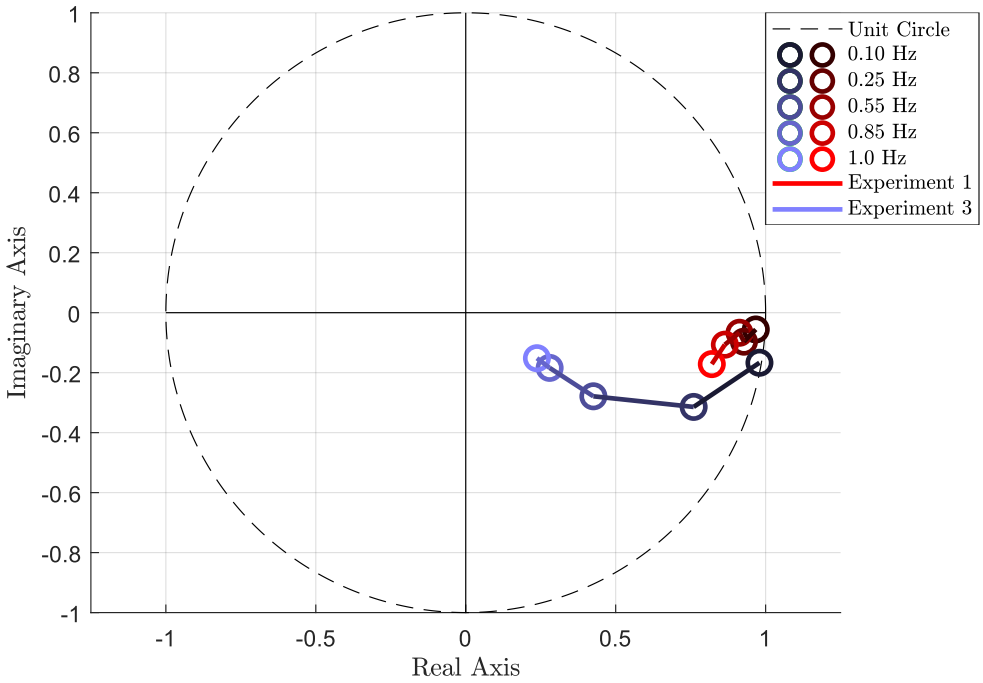

Figure 4.12: Comparison of system responses on a complex plane between Experiment 1 and Experiment 3, tracking of predictable input with (shades of red) versus without (shades of blue) direct visual feedback. Each circle corresponds to the response at stimulus frequencies, the darkest shade for the smallest frequency and the lightest shade for the largest frequency component of the experiments. The unit circle symbolizes the perfect tracking with gain one as a reference point, and the positive real axis represents the perfect phase with zero lag.

Building on these observations, the nature of the visual feedback provided to the subjects in the two experiments leads to distinct behavioral and performance outcomes. In Experiment 1, where subjects receive direct visual feedback from both the target and their position, the system can be likened to a closed-loop control system with full-state feedback from an engineering standpoint. This direct feedback allows immediate and intuitive corrections, resulting in a more linear and predictable system. Suggesting that the human motor system, when equipped with comprehensive information, can effectively minimize tracking errors, leading to a more stable response. Conversely, in Experiment 3, the absence of direct positional feedback might cause the brain to rely more on memory and prediction, introducing elements of uncertainty.

The observed Mean Squared Error (MSE) trends presented in Fig. 4.13 further accentuate these differences. The relatively consistent MSE across repeated trials in Experiment 1 suggests a stable system response. In contrast, the drastic changes in MSE between repeated trials in Experiment 3 indicate a system with higher variance and potentially less predictability. This variability underscores the profound impact of feedback mechanisms on system performance and stability, highlighting the intricate interplay between engineering principles and biological systems in human tracking tasks. Increasing MSE with frequency for both experiments indicates the challenges in tracking as the input frequency rises, which we could attribute to the inherent limitations in the human motor system's bandwidth.

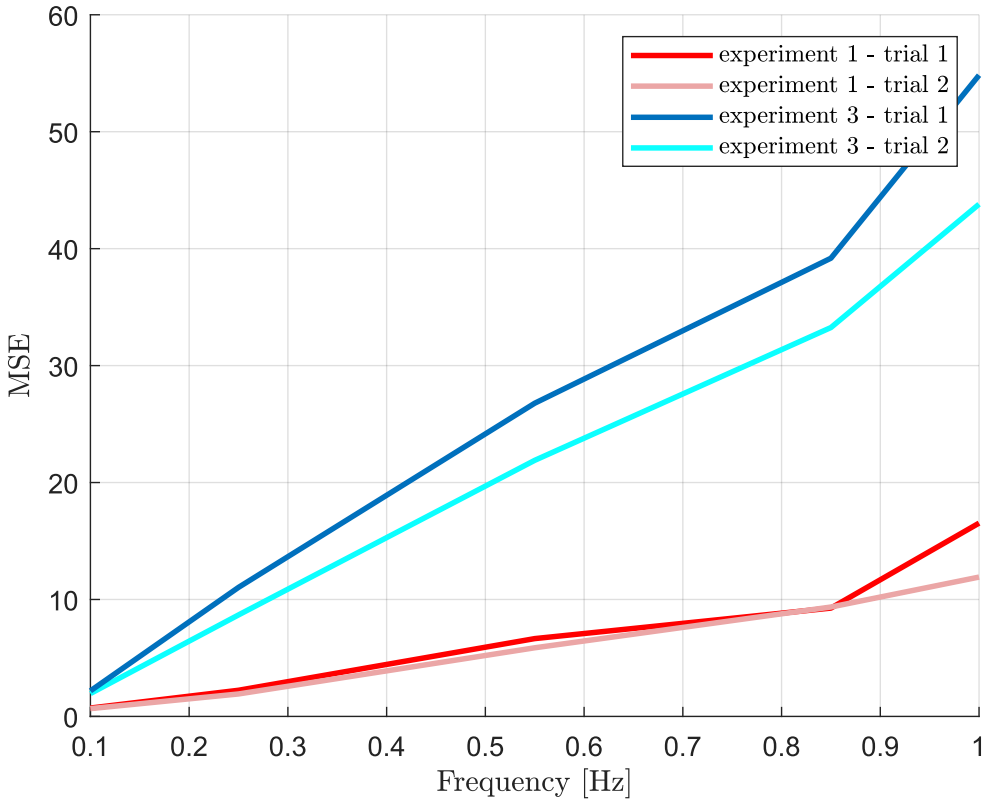

Figure 4.13: Comparison of mean squared error between trials for Experiment 1 and Experiment 3, dark red line depicts the first trial for Experiment 1 while the light red signal represents the second trial. Similarly, the dark blue signal depicts the first trial in Experiment 3, while the light blue represents the second trial.

Suppose we interpret the outcomes from the biological view, while the initial performance in Experiment 3 is inferior due to the lack of direct visual feedback. In that

case, the human motor system is known for its adaptability. Relying solely on error feedback might have forced subjects to pay more attention to their performance and adapt more quickly to reduce the error, resulting in a steeper learning curve and a more rapid decrease in tracking error over repeated trials. Also, the decline in overall performance could result from cognitive load. Experiment 1 might have a lower cognitive load since subjects can directly see and follow the target. In contrast, Experiment 3 might impose a higher cognitive load as subjects need to interpret the error signal and adjust their movements accordingly.

In summary, the critical difference between the two experiments is the type of feedback provided, which can have significant implications for motor adaptation, learning, cognitive load, and the cerebellum's role in these processes. Analyzing the results from these experiments can provide insights into how different feedback mechanisms influence motor control and adaptation.

4.4 Comparison Between Experiment 3 and Experiment 4 (Predictable vs. Unpredictable Input Without Direct Visual Feedback)

We used the same scene for Experiment 3 and Experiment 4 and created variations of compensatory control tasks. These two experiments differ in introduced input signals. In Experiment 3, participants were subjected to track several single-frequency sinusoidal signal inputs, while in Experiment 4, they encountered a sum-of-sine signal. This difference in input complexity is reflected in their complex domain characterizations given in Fig. 4.15 and magnitude and phase responses given in Fig. 4.14.

For Experiment 3, the magnitude response starts relatively high at lower frequencies. Then, it attenuates as the frequency increases, suggesting that participants could track the target effectively at lower frequencies, but their performance declined at higher frequencies. The phase response shows a consistent lag across the frequency spectrum, indicating a delay in participants' reactions, which is expected given the absence of direct positional feedback. On the other hand, Experiment 4's magnitude response is considerably lower across all frequencies compared to Experiment 3, indicating a reduced ability to track the target, especially given the more complex

sum-of-sines input. The phase response for Experiment 4 also exhibits a more pronounced lag, especially at higher frequencies, suggesting that the participants found it even more challenging to synchronize their movements with the target's trajectory.

We can attribute the differences in magnitude and phase responses between the two experiments to the inherent challenges of tracking a more complex and unpredictable input signal in Experiment 4. The sum-of-sine signal input introduces multiple frequency components, making it harder for participants to anticipate and respond to target movements, especially without direct positional feedback.

Biologically, the brain's ability to process and react to sensory information might be overwhelmed by the unpredictability of the sum-of-sine signal input in Experiment 4. Without direct visual feedback, participants rely more on internal models and predictions. The added complexity of the input signal in Experiment 4 could disrupt these internal models, leading to decreased tracking accuracy and increased phase lag.

In summary, while both Experiment 3 and Experiment 4 deprived participants of direct positional feedback, the added complexity of the sum-of-sine signal in Experiment 4 further challenged the participants' tracking abilities, as evidenced by the Bode plot responses. This outcome further highlights the intricate balance between input complexity and the availability of feedback in determining human performance in tracking tasks.

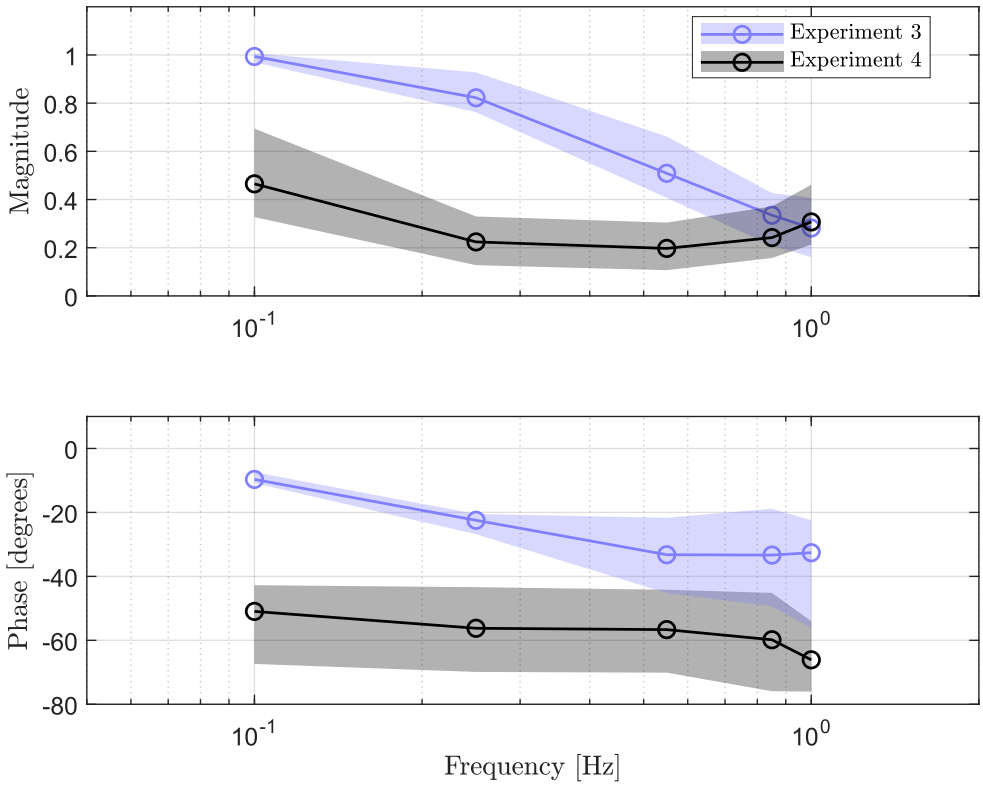

Figure 4.14: Comparison of magnitude and phase responses between Experiment 3 and Experiment 4, tracking of predictable input (blue) versus unpredictable input (black) without direct visual feedback. The solid lines represent the mean response, while the same colored transparent bounds correspond to the confidence region calculated between the first and last quartile for respective experiments.

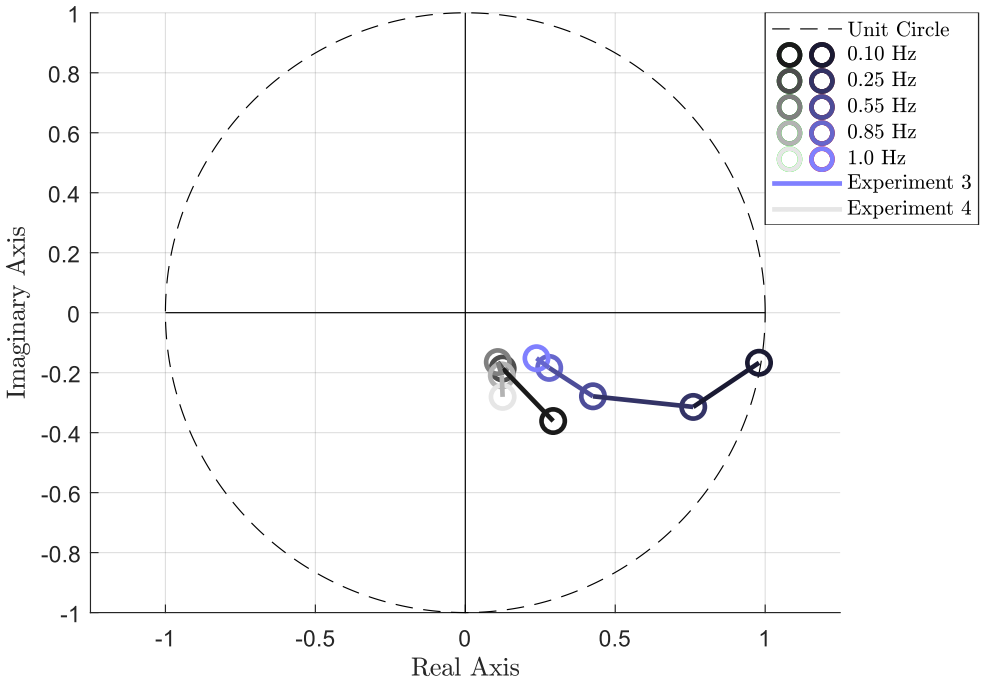

Figure 4.15: Comparison of system responses on a complex plane between Experiment 3 and Experiment 4, tracking of predictable input (shades of blue) versus unpredictable input (shades of black) without direct visual feedback. Each circle corresponds to the response at stimulus frequencies, the darkest shade for the smallest frequency and the lightest shade for the largest frequency component of the experiments. The unit circle symbolizes the perfect tracking with gain one as a reference point, and the positive real axis represents the perfect phase with zero lag.

4.5 Comparison Between Experiment 2 and Experiment 4 (Unpredictable Input With vs. Without Direct Visual Feedback)

Both Experiment 2 and Experiment 4 utilized a sum-of-sine signal input, but they were presented to participants with different visual feedback scenarios. In Experiment 2, participants had direct visual feedback of the target and their position, while in Experiment 4, this direct feedback was absent. The Bode plot responses and complex plane characterizations of both experiments are shown in Fig. 4.16 and Fig. 4.17 respectively.

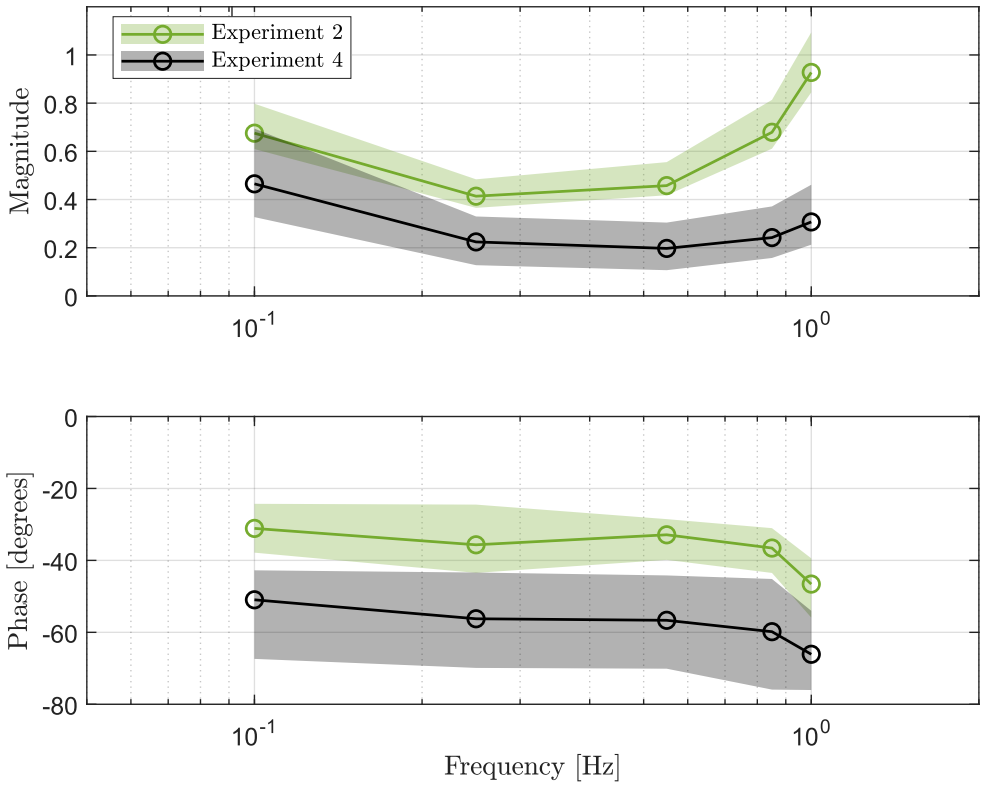

Figure 4.16: Comparison of magnitude and phase responses between Experiment 2 and Experiment 4, tracking of unpredictable input with (green) versus without (black) direct visual feedback

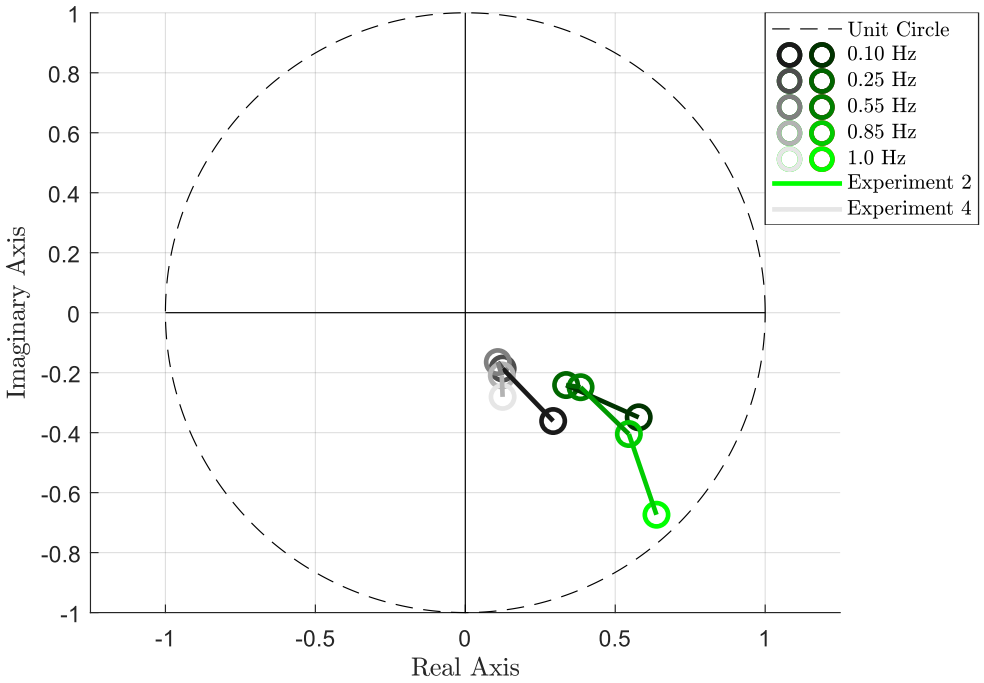

Figure 4.17: Comparison of system responses on a complex plane between Experiment 2 and Experiment 4, tracking of unpredictable input with (shades of green) versus without (shades of black) direct visual feedback. Each circle corresponds to the response at stimulus frequencies, the darkest shade for the smallest frequency and the lightest shade for the largest frequency component of the experiments. The unit circle symbolizes the perfect tracking with gain one as a reference point, and the positive real axis represents the perfect phase with zero lag.

The phase response for both experiments shows a lag. However, it is more pronounced in Experiment 4, suggesting that, without direct visual feedback, participants in Experiment 4 experienced a more significant delay in their reactions to the target's movements.

The magnitude responses of both experiments shown in Fig. 4.16 exhibit a notable "U" shape or notch filter-like behavior. This characteristic shape suggests that the system (in this case, the human subjects) attenuates specific frequencies more than others. The more pronounced response around 1 Hz might indicate a resonance or a frequency at which the human motor system is most responsive or sensitive.

Observing a notch filter-like magnitude response in Experiment 2 and 4 is intriguing

and can be attributed to various factors. Explanation can be made from both biological and methodological views. From the biological point of view, this outcome might arise from the inherently adaptive mechanisms of the human sensory-motor system. When faced with a sum-of-sine input, specific frequencies might be more challenging for the brain to process and track, leading to a reduced response, creating a "notch" in the frequency response where the system's tracking ability is diminished. Another reason could be neural resonance. Just as mechanical systems have resonant frequencies, neural circuits can also exhibit resonance-like behaviors. The frequencies around the notch may be more challenging for the brain to process due to some form of neural resonance or interference.

From the engineering point of view, his phenomenon could result from the predominant noise around the 1 Hz frequency during data collection. This type of noise characteristic might artificially inflate the response at this frequency, making it appear as if the response is better, thereby creating a notch-like appearance. In Fig. 4.18, we give the responses at the stimulus frequencies with blue and noise content with orange. To explicitly investigate the noise content we got rid of the response at stimulus frequencies. In Fig. 4.19, we see the general trend of noise on a wider frequency range, decreasing as the frequency increases. Fig. 4.20 zooms to the focused frequency range. In this figure, we do not see any indications of a suspected noise pattern creating a false response, which makes the biological explanations more credible.

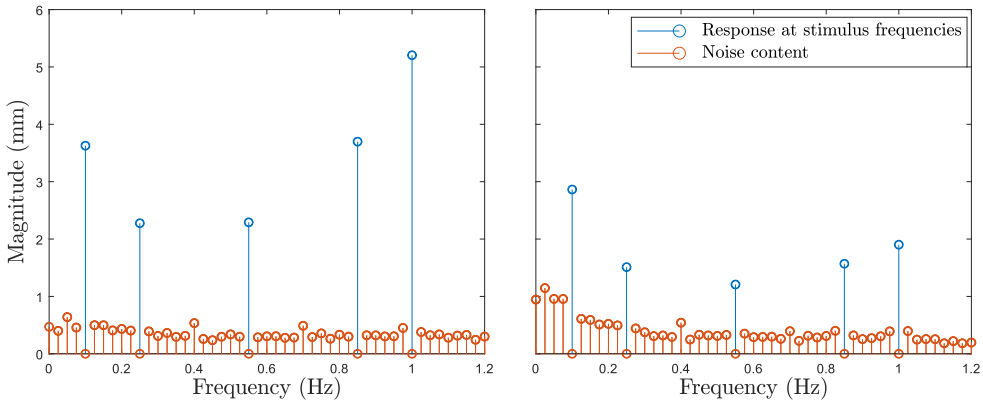

Figure 4.18: FFT results of Experiment 2 (left) and Experiment 4 (right). The blue lines correspond to the stimulus frequencies.

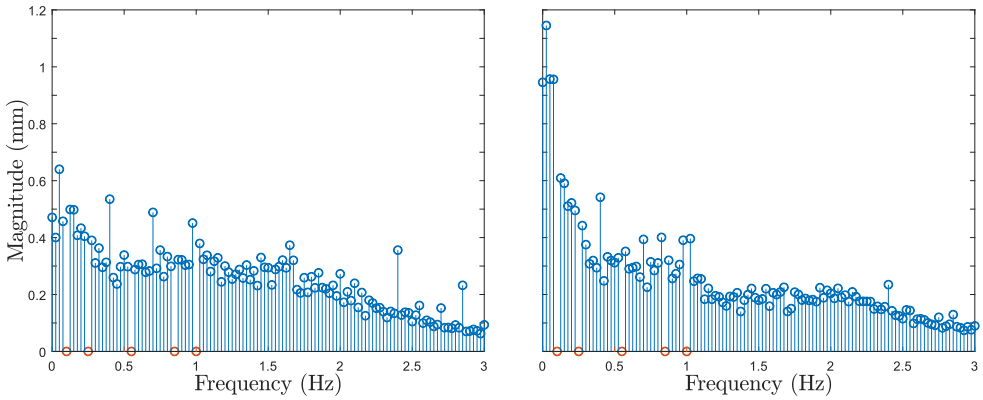

Figure 4.19: Noise content extracted from FFT of Experiment 2 (left) and Experiment 4 (right) up to 3 Hz to observe the general noise trend. Orange circles correspond to the stimulus frequencies.

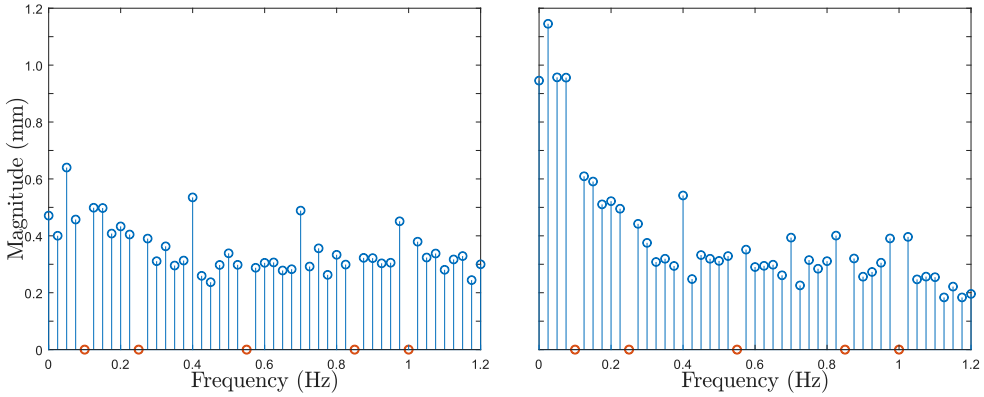

Figure 4.20: Noise content extracted from FFT of Experiment 2 (left) and Experiment 4 (right) up to 1.2 Hz to closely see the trend around the stimulus frequencies. Orange circles correspond to the stimulus frequencies.

The difference in Bode plot responses between the two experiments underscores the importance of feedback mechanisms in tracking systems. Direct visual feedback in Experiment 2 likely provided participants with a reference point, aiding error correction and enhancing their tracking performance. Without this feedback in Experiment 4, participants had to rely solely on feedback, leading to decreased tracking accuracy and increased phase lag.

Biologically, direct visual feedback in Experiment 2 would have engaged the partic-

ipants' visual processing pathways, allowing for real-time adjustments and corrections. Without this feedback, in Experiment 4, participants had to rely more heavily on proprioceptive feedback, which might not be as effective for complex, multi-frequency inputs like the sum-of-sine signals.

In conclusion, while both Experiment 2 and Experiment 4 subjected participants to the same sum-of-sine input, the presence or absence of direct visual feedback played a crucial role in their tracking performance. The Bode plot responses highlight the challenges posed by complex inputs, mainly when feedback mechanisms are limited or absent.

4.6 Discussion

Using the first experimental scene, Experiment 1 and Experiment 2 create versions of the pursuit control task presented in [31]. If we model this scene on a state space, naming our state vector as Z_p, our states would be:

$$Z_p = \begin{bmatrix} x \\ \dot{x} \\ r \\ \dot{r} \\ e \\ \dot{e} \end{bmatrix} \tag{4.1}$$

On the other hand, Experiment 3 and Experiment 4 create versions of compensatory control tasks presented in the same research using the second experimental scene. If we model this scene using a state space, naming our state vector Z_c, our states would be:

$$Z_c = \begin{bmatrix} e \\ \dot{e} \end{bmatrix} \tag{4.2}$$

In this second experimental scene, the only source of feedback is the position er-

ror, which creates a reactive control task. Humans cannot measure their motor command output; other than the error, the system's states are unobservable. The compensatory display control model is often represented with a simple closed-loop diagram in Fig. 4.21.

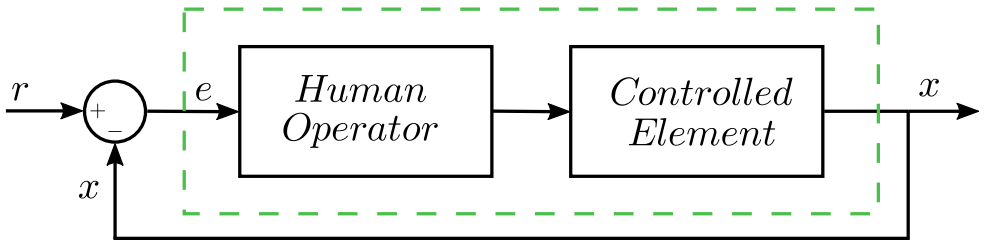

Figure 4.21: Block diagram for the compensatory control model.

Access to position and velocity information of both the input and the output, along with the error position and velocity, creates a better observer in the first experimental scene. Since two copies of the same information correcting each other are present within the observer, the error is corrected using other states' information and feedback. This phenomenon creates a better overall control with both predictive and reactive components. In this scene, the reactive component is suggested to be the same controller in the compensatory display [32]. In contrast, the predictive component is commonly modeled with a feedforward component [34, 36, 37, 38]. Here, we suggest to model the effect of input and output separately. In Fig. 4.22, FF_x is the feedforward model of the effect of having the state information and an estimation of motor commands of the operator. FF_r is for the feedforward model of directly seeing the target.

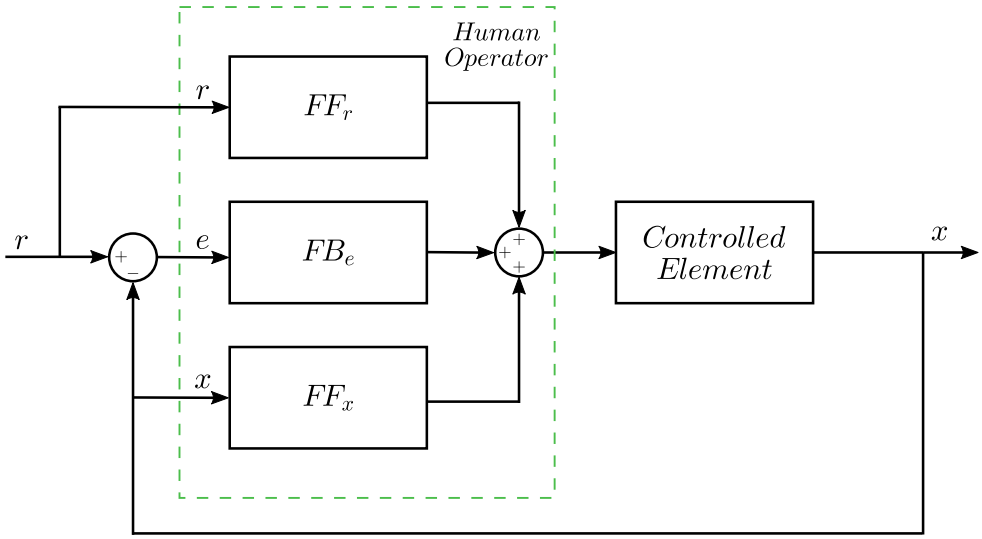

Figure 4.22: Block diagram for the pursuit control model.

The body is assumed to voluntarily create redundancy in biology, collecting and merging various sensory information to achieve the best prediction and control [50, 51]. Having complete state information in the pursuit control task creates similar redundancy. In this scene, we hypothesize that humans could be using their internal model predictor (IMP) regardless of the input type since they can predict the output of their own motor command. However, we still see a decrease in performance between Experiment 1 and Experiment 2, suggesting that IMP becomes less functional based on the input's predictability.

Humans' IMP works on experience basis [52, 53, 54, 55] and can be considered the source of feedforward models in systems [56]. In our last hypothesis, we mentioned that IMP could be affected by the predictability property of the input, suggesting that predictable inputs increase the prediction ability and create experience since they give insight into the future of input. We can now ask how the IMP performance changes for different feedbacks given predictable inputs. If we compare Experiment 1 and Experiment 3, where the inputs have predictable patterns, responses are close to each other at lower frequencies yet significantly differ at higher frequencies. This outcome could suggest that the compensatory control could still be under the influence of IMP at lower frequencies, and consequently, we might be able to mention feedforward models for predictable inputs at lower frequencies. However, it is crucial to point at

higher frequencies, performance gradually decreases for Experiment 3, suggesting a bandwidth to IMP at this compensatory control case.

Another critical deduction can be the frequency sensitivity of IMP. Even with predictable input and perfect state knowledge demonstrated in the pursuit control task in Experiment 1, we see a decay in performance as the frequency increases, suggesting a bandwidth limit to IMP and feedforward control, similar to the findings in [38]. However, this pursuit control bandwidth can be considered broader compared to the compensatory control task in Experiment 3.

Up to this point, we discussed the effects of input and feedback on IMP. We can also look into which aspect the IMP relies more heavily on by comparing Experiments 1, 2, and 3 together. In Experiment 1, we have perfect feedback with predictable input. Experiment 2 differs in input, while Experiment 3 separates from Experiment 1 in feedback states. As seen from Fig. 4.24, mean MSE is lowest for Experiment 1, as expected. However, contrary to our expectations, the second lowest mean MSE level is presented for Experiment 3 and the highest MSE levels, and consequently, the worst performance is observed for Experiment 2.

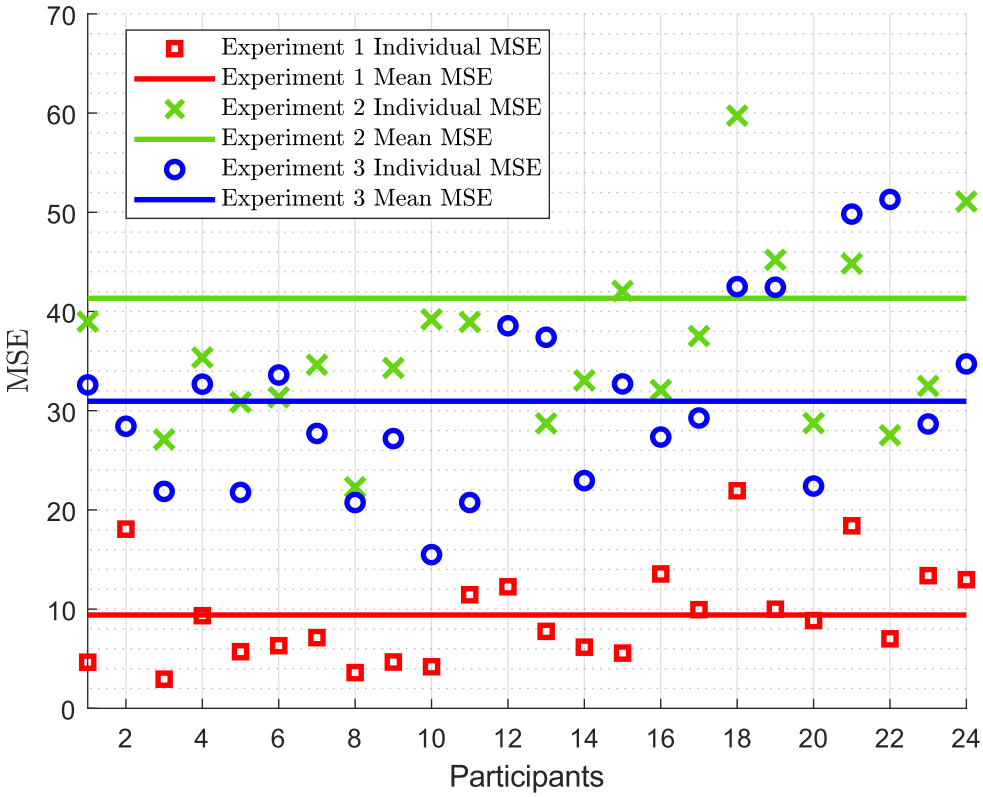

Figure 4.23: We give mean MSE results for each participant and the overall mean MSE for Experiments 1 (red), 2 (green), and 3 (blue). For Experiments 1 and 3, we calculate the mean MSE by taking the mean of every single-frequency performance.

This outcome might suggest that the IMP relies more on the input's predictability, and even with restricted state feedback, it helps to display accurate performance. Another reason might be the frequency range of experiments. As seen from both united Bode plot 4.24 and complex plane Fig. 4.25 response representations, it is clear that the predictable input magnitude response of Experiment 3 is significantly better than Experiment 2 at lower frequencies, and phase response is better at every frequency. However, we see a significantly better magnitude response at higher frequencies in Experiment 2. This outcome could have changed if we increased the frequency range since, as we discussed, IMP seems to have a bandwidth property. In a broader frequency range, the feedback states might be prevailing.

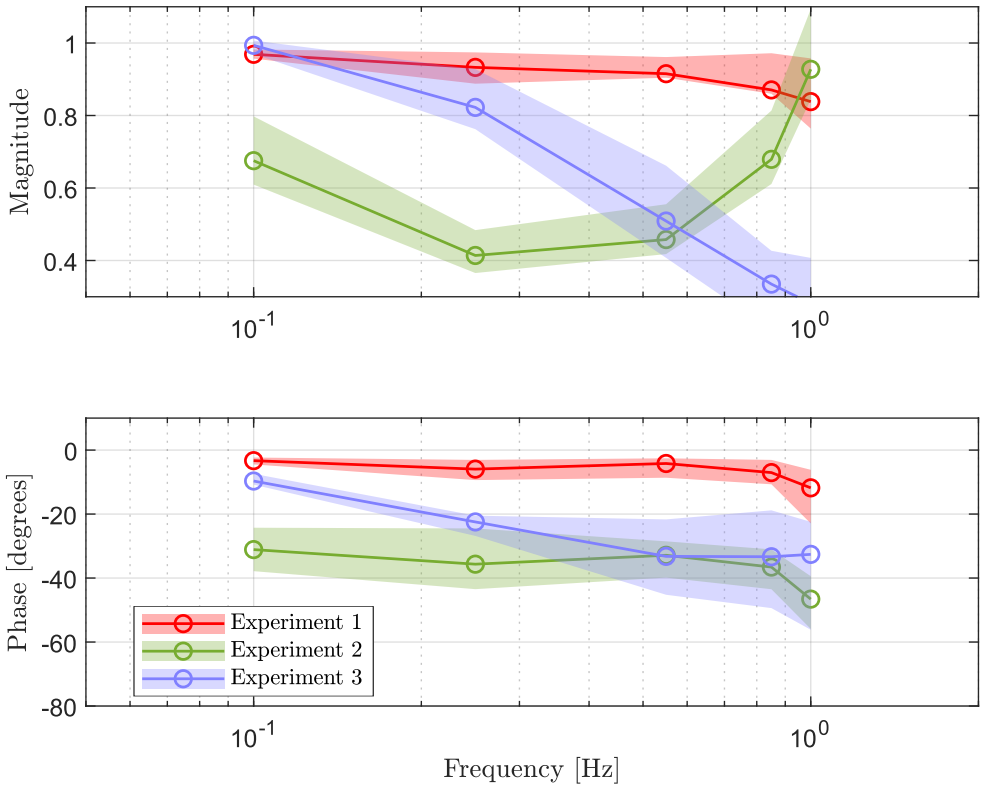

Figure 4.24: Comparison of magnitude and phase responses between Experiment 1 (red), 2 (green), and 3 (blue), tracking of predictable input with direct feedback, unpredictable input with direct feedback, and predictable input without direct visual feedback. The solid lines represent the mean response, while the same colored transparent bounds correspond to the confidence region calculated between the first and last quartile for respective experiments.

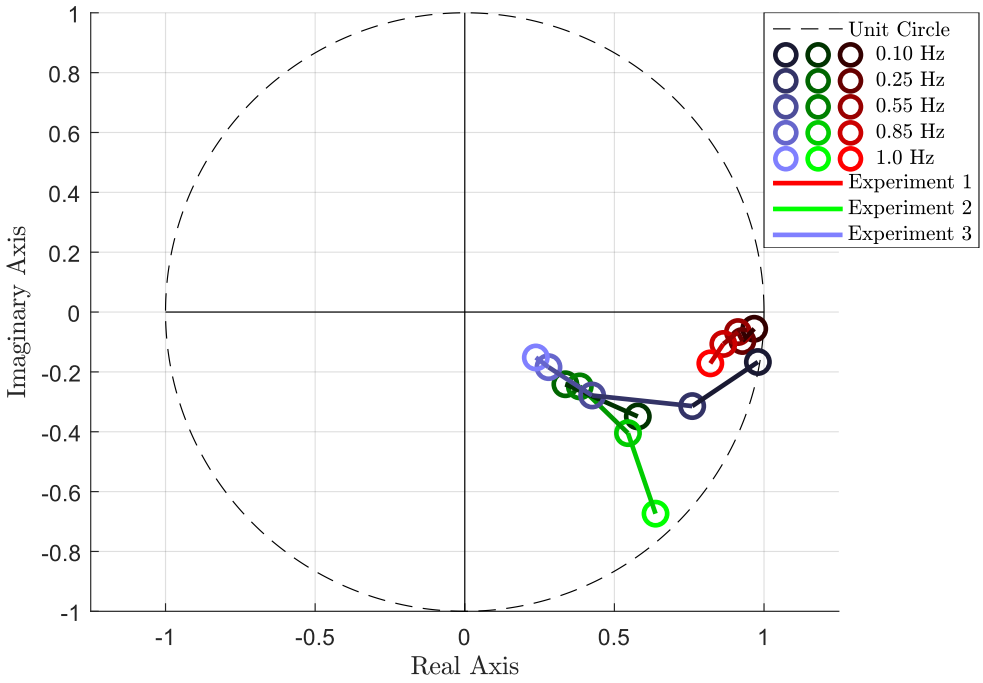

Figure 4.25: Comparison of system responses on a complex plane between Experiment 1 (shades of red), 2 (shades of green), and 3 (shades of blue), tracking of predictable input with direct feedback, unpredictable input with direct feedback, and predictable input without direct visual feedback. Each circle corresponds to the response at stimulus frequencies, the darkest shade for the smallest frequency and the lightest shade for the largest frequency component of the experiments. The unit circle symbolizes the perfect tracking with gain one as a reference point, and the positive real axis represents the perfect phase with zero lag.

Regardless of which experiment we conducted, the best responses were almost always at the lowest frequency, suggesting a frequency sensitivity for the tracking task. However, unexpectedly, we saw an improved trend in the extreme frequencies for the cases with unpredictable inputs. This observation can be attributed to various factors, both biological and methodological. From the biological point of view, it might be caused by the inherently adaptive mechanisms of the human sensory-motor system. When faced with a sum-of-sine signal input, specific frequencies might be more challenging for the brain to process and track, leading to a reduced response. Another reason could be neural resonance. Just as mechanical systems have resonant frequencies, neural circuits can also exhibit resonance-like behaviors. From the engineering

point of view, we suspected a predominant noise presence around 1 Hz frequency during data collection that could artificially inflate the response at this frequency, making it appear as if there is a higher response, thereby creating a notch-like appearance in the surrounding frequencies. However, upon analyzing the respective figures discussed earlier, we could not find any evidence of this phenomenon. We concluded that the shared "U" shape in magnitude response across the two experiments probably suggests inherent properties of the human motor system.

CHAPTER 5

CONCLUSION AND FUTURE WORK

5.1 Conclusion

This research offers a comprehensive exploration into the adaptability and responsiveness of the human sensory-motor system, especially in tracking tasks. Rooted in the pursuit and compensatory control models presented in [31], the experiments consistently highlighted the profound influence of feedback mechanisms and input predictability on performance.

In the pursuit control tasks of the initial experiments, direct visual feedback provided participants with a perfect observer, facilitating both predictive and reactive control components. This dual control mechanism, characteristic of biological systems, ensures optimal performance despite unpredictable stimuli. The transition from Experiment 1 to Experiment 2 illustrates the challenges introduced by unpredictable inputs, even when participants are equipped with full-state feedback.

The Internal Model Predictor (IMP) operates based on past experiences. In scenarios like Experiments 1 and 2, where participants can anticipate the outcome of their motor commands, the IMP is actively engaged. However, its effectiveness decreases with unpredictable inputs, as shown by the performance difference between Experiments 1 and 2. It suggests that while the IMP is good at tracking predictable inputs, its ability drops when faced with complex, unpredictable stimuli, even with comprehensive feedback. Moreover, performance declines with increasing frequency even in scenarios characterized by perfect predictability and feedback, such as Experiment 1. This decline suggests an inherent bandwidth limit to the IMP and feedforward control, emphasizing the challenges of high-frequency tracking tasks.

Most related works in Chapter 1 recreate the pursuit control task, providing global variables to the operators. This is not a realistic approach to recreating real-life scenarios. For instance, while potentially observing a reference target, pilots frequently lack comprehensive knowledge of their own state. Similarly, in the tracking tasks of weakly electric fish, the fish, even in well-lit environments, often only know the refuge's position, remaining unaware of their position [57]. Despite being able to observe the input signal in both scenarios, they interpret it based on perceived errors, mainly because they lack awareness of their state. This research, diverging from conventional literature, meticulously implemented and tested both the compensatory control task, as presented in [31], and the pursuit control task, offering a more nuanced and layered understanding of these models. For example, our compensatory control task reflects the experiments done with weakly electric fish in dark settings, simulating a stabilization challenge.

We encountered a shared "U" shaped magnitude response across unpredictable stimulus experiments, potentially hinting at inherent properties of the human motor system. Still waiting to be discovered, this phenomenon could result from several biological factors, such as neural resonance.

This research provides a comprehensive understanding of the capabilities and limitations inherent to the human sensory-motor system in tracking tasks. The findings highlight the critical importance of feedback mechanisms, input predictability, and frequency sensitivity in shaping performance. These insights deepen our understanding of human motor control and pave the way for the design of systems that effectively interact with or augment human capabilities.

5.2 Future work

In future studies, there are several promising areas to explore. We see a decay in performance as the frequency increases, which indicates that experiments create a challenge for the subjects, yet one main improvement would be to expand the frequency range. By doing this, we could get a better and more complete understanding of the topic, perhaps finding important details that the current frequency range might

miss.

Another important aspect is to include a broader range of participants from different age groups and backgrounds and those with different health conditions. It would also be interesting to compare our results with those of professionals, like surgeons or pilots, who have special training that might give them different sensory feedback skills.

A significant factor that can impact results is the cognitive load. Tracking an unpredictable sum-of-sine signal trajectory can be more mentally taxing than a single sine wave, which might lead to reduced performance. At this point, a critical question in research can be how cognitive load, which is caused by unpredictable trajectories, affects motor performance and adaptation. To investigate this, a potential study could add a secondary cognitive task, such as a simple math problem, while participants perform a tracking task. By comparing performance under these dual-task conditions to single-task conditions, we could gain insights into the cognitive resources utilized for motor adaptation.

On the technical side, testing subjects on a 2D trajectory would add another layer to the experiment and might reveal new findings about how people handle more complex tasks. Finally, haptic feedback's effect on a tracking task is an area we have yet to look into. By adding haptic feedback to our experiments, we could get closer to understanding how it might be used in real-world settings, especially in jobs like piloting, where feeling and reacting to feedback is crucial.

REFERENCES

[1] M. H. Dickinson, C. T. Farley, R. J. Full, M. Koehl, R. Kram, and S. Lehman, "How animals move: an integrative view," *science*, vol. 288, no. 5463, pp. 100–106, 2000.

[2] T. Kiemel, Y. Zhang, and J. J. Jeka, "Identification of neural feedback for upright stance in humans: stabilization rather than sway minimization," *Journal of Neuroscience*, vol. 31, no. 42, pp. 15144–15153, 2011.

[3] N. J. Cowan, M. M. Ankarali, J. P. Dyhr, M. S. Madhav, E. Roth, S. Sefati, S. Sponberg, S. A. Stamper, E. S. Fortune, and T. L. Daniel, "Feedback control as a framework for understanding tradeoffs in biology," *American Zoologist*, vol. 54, no. 2, pp. 223–237, 2014.

[4] B. R. Umberger and R. H. Miller, "Optimal control modeling of human movement," *Handbook of human motion*, pp. 327–348, 2018.

[5] A. M. Mert, S. Sefati, M. S. Madhav, A. Long, A. J. Bastian, and N. J. Cowan, "Walking dynamics are symmetric (enough)," *Journal of the Royal Society Interface*, vol. 12, no. 108, p. 20150209, 2015.

[6] I. Uyanik, S. Sefati, S. A. Stamper, K.-A. Cho, M. M. Ankarali, E. S. Fortune, and N. J. Cowan, "Variability in locomotor dynamics reveals the critical role of feedback in task control," *Elife*, vol. 9, p. e51219, 2020.

[7] S. Sefati, I. D. Neveln, E. Roth, T. R. Mitchell, J. B. Snyder, M. A. MacIver, E. S. Fortune, and N. J. Cowan, "Mutually opposing forces during locomotion can eliminate the tradeoff between maneuverability and stability," *Proceedings of the national academy of sciences*, vol. 110, no. 47, pp. 18798–18803, 2013.

[8] E. Roth, S. Sponberg, and N. Cowan, "A comparative approach to closed-loop computation," *Current opinion in neurobiology*, vol. 25, pp. 54–62, 2014.

[9] M. S. Madhav and N. J. Cowan, "The synergy between neuroscience and control theory: the nervous system as inspiration for hard control challenges," *Annual Review of Control, Robotics, and Autonomous Systems*, vol. 3, pp. 243–267, 2020.

[10] S. Ravi, R. Noda, S. Gagliardi, D. Kolomenskiy, S. Combes, H. Liu, A. A. Biewener, and N. Konow, "Modulation of flight muscle recruitment and wing rotation enables hummingbirds to mitigate aerial roll perturbations," *Current Biology*, vol. 30, no. 2, pp. 187–195, 2020.

[11] M. M. Ankarali, H. Tutkun Sen, A. De, A. M. Okamura, and N. J. Cowan, "Haptic feedback enhances rhythmic motor control by reducing variability, not improving convergence rate," *Journal of Neurophysiology*, vol. 111, no. 6, pp. 1286–1299, 2014.

[12] C. P. Smith and R. F. Reynolds, "Vestibular feedback maintains reaching accuracy during body movement," *The Journal of Physiology*, vol. 595, no. 4, pp. 1339–1349, 2017.

[13] S. Sponberg, J. P. Dyhr, R. W. Hall, and T. L. Daniel, "Luminance-dependent visual processing enables moth flight in low light," *Science*, vol. 348, no. 6240, pp. 1245–1248, 2015.

[14] D. Biswas, A. Lamperski, Y. Yang, K. Hoffman, J. Guckenheimer, E. S. Fortune, and N. J. Cowan, "Organisms use mode-switching to solve the explore-vs-exploit problem," *bioRxiv*, pp. 2023–01, 2023.

[15] A. N. Peterson, A. P. Soto, and M. J. McHenry, "Pursuit and evasion strategies in the predator–prey interactions of fishes," *Integrative and comparative biology*, vol. 61, no. 2, pp. 668–680, 2021.

[16] C.-S. Yu, E. M.-y. Wang, W.-C. Li, G. Braithwaite, and M. Greaves, "Pilots' visual scan patterns and attention distribution during the pursuit of a dynamic target," *Aerospace medicine and human performance*, vol. 87, no. 1, pp. 40–47, 2016.

[17] W.-C. Li, C.-S. Yu, G. Braithwaite, and M. Greaves, "Pilots' attention distri-

butions between chasing a moving target and a stationary target," *Aerospace medicine and human performance*, vol. 87, no. 12, pp. 989–995, 2016.

[18] M. T. Gettman, M. L. Blute, G. K. Chow, R. Neururer, G. Bartsch, and R. Peschel, "Robotic-assisted laparoscopic partial nephrectomy: technique and initial clinical experience with davinci robotic system," *Urology*, vol. 64, no. 5, pp. 914–918, 2004.

[19] A. E. Abdelaal, P. Mathur, and S. E. Salcudean, "Robotics in vivo: A perspective on human–robot interaction in surgical robotics," *Annual Review of Control, Robotics, and Autonomous Systems*, vol. 3, pp. 221–242, 2020.

[20] M. Nakayama, F. C. Holsinger, D. Chevalier, and R. K. Orosco, "The dawn of robotic surgery in otolaryngology-head and neck surgery," *Japanese journal of clinical oncology*, vol. 49, no. 5, pp. 404–411, 2019.

[21] K. Ryokai, F. Farzin, E. Kaltman, and G. Niemeyer, "Assessing multiple object tracking in young children using a game," *Educational Technology Research and Development*, vol. 61, pp. 153–170, 2013.

[22] W. R. Boot, A. F. Kramer, D. J. Simons, M. Fabiani, and G. Gratton, "The effects of video game playing on attention, memory, and executive control," *Acta psychologica*, vol. 129, no. 3, pp. 387–398, 2008.

[23] K. E. Barrett, S. M. Barman, H. L. Brooks, and J. X.-J. Yuan, *Excitable Tissue: Nerve*. New York, NY: McGraw-Hill Education, 2019.

[24] K. E. Barrett, S. M. Barman, H. L. Brooks, and J. X.-J. Yuan, *Excitable Tissue: Muscle*. New York, NY: McGraw-Hill Education, 2019.

[25] K. E. Barrett, S. M. Barman, S. Boitano, and J. F. Reckelhoff, *Reflex; Voluntary Control of Posture; Movement*. New York, NY: McGraw-Hill Education, 2017.

[26] R. W. Nickl, M. M. Ankarali, and N. J. Cowan, "Complementary spatial and timing control in rhythmic arm movements," *Journal of neurophysiology*, vol. 121, no. 4, pp. 1543–1560, 2019.

[27] E. Roth, R. W. Hall, T. L. Daniel, and S. Sponberg, "Integration of parallel mechanosensory and visual pathways resolved through sensory conflict," *Pro-*

ceedings of the National Academy of Sciences, vol. 113, no. 45, pp. 12832–12837, 2016.

[28] B. Mehta and S. Schaal, "Forward models in visuomotor control," *Journal of Neurophysiology*, vol. 88, no. 2, pp. 942–953, 2002.

[29] L. Li, R. Chen, and J. Chen, "Playing action video games improves visuomotor control," *Psychological science*, vol. 27, no. 8, pp. 1092–1108, 2016.

[30] M. Noble, P. M. Fitts, and C. E. Warren, "The frequency response of skilled subjects in a pursuit tracking task.," *Journal of Experimental Psychology*, vol. 49, no. 4, p. 249, 1955.

[31] E. S. Krendel and D. T. McRuer, "A servomechanisms approach to skill development," *Journal of the Franklin Institute*, vol. 269, no. 1, pp. 24–42, 1960.

[32] D. T. McRuer and H. R. Jex, "A review of quasi-linear pilot models," *IEEE transactions on human factors in electronics*, no. 3, pp. 231–249, 1967.

[33] R. J. Wasicko, D. T. McRuer, and R. E. Magdaleno, *Human pilot dynamic response in single-loop systems with compensatory and pursuit displays*, vol. 66. Air Force Flight Dynamics Laboratory, Research and Technology Division, Air . . . , 1966.

[34] F. M. Drop, D. M. Pool, H. J. Damveld, M. M. van Paassen, and M. Mulder, "Identification of the feedforward component in manual control with predictable target signals," *IEEE transactions on cybernetics*, vol. 43, no. 6, pp. 1936–1949, 2013.

[35] H. Ohtsuka, K. Shibasato, and S. Kawaji, "A perceptual motor control model based on output feedback adaptive control theory," in *ICINCO-RA*, 2016.

[36] X. Zhang, S. Wang, J. B. Hoagg, and T. M. Seigler, "The roles of feedback and feedforward as humans learn to control unknown dynamic systems," *IEEE transactions on cybernetics*, vol. 48, no. 2, pp. 543–555, 2017.

[37] E. Roth, D. Howell, C. Beckwith, and S. A. Burden, "Toward experimental validation of a model for human sensorimotor learning and control in teleop-

eration," in *Micro-and Nanotechnology Sensors, Systems, and Applications IX*, vol. 10194, pp. 380–391, SPIE, 2017.

[38] M. Yamagami, D. Howell, E. Roth, and S. A. Burden, "Contributions of feedforward and feedback control in a manual trajectory-tracking task," *IFAC-PapersOnLine*, vol. 51, no. 34, pp. 61–66, 2019.

[39] B. Yu, R. B. Gillespie, J. S. Freudenberg, and J. A. Cook, "Human control strategies in pursuit tracking with a disturbance input," in *53rd IEEE Conference on Decision and Control*, pp. 3795–3800, IEEE, 2014.

[40] F. R. Danion, J. Mathew, N. Gouirand, and E. Brenner, "More precise tracking of horizontal than vertical target motion with both the eyes and hand," *Cortex*, vol. 134, pp. 30–42, 2021.

[41] M. Yamagami, L. N. Peterson, D. Howell, E. Roth, and S. A. Burden, "Effect of handedness on learned controllers and sensorimotor noise during trajectory-tracking," *IEEE Transactions on Cybernetics*, 2021.

[42] L. N. Peterson, A. H. Chou, S. A. Burden, and M. Yamagami, "Assessing human feedback parameters for disturbance-rejection," *IFAC-PapersOnLine*, vol. 55, no. 41, pp. 1–6, 2022.

[43] C. S. Yang, N. J. Cowan, and A. M. Haith, "De novo learning versus adaptation of continuous control in a manual tracking task," *elife*, vol. 10, p. e62578, 2021.

[44] S. A. S. Mousavi, X. Zhang, T. M. Seigler, and J. B. Hoagg, "Characteristics that make linear time-invariant dynamic systems difficult for humans to control," *IEEE Transactions on Human-Machine Systems*, vol. 51, no. 2, pp. 141–151, 2021.

[45] M. G. Parker, A. P. Weightman, S. F. Tyson, B. Abbott, and W. Mansell, "Sensorimotor delays in tracking may be compensated by negative feedback control of motion-extrapolated position," *Experimental brain research*, vol. 239, pp. 189–204, 2021.

[46] E. Roth, K. Zhuang, S. A. Stamper, E. S. Fortune, and N. J. Cowan, "Stimulus predictability mediates a switch in locomotor smooth pursuit performance

for eigenmannia virescens," *Journal of experimental biology*, vol. 214, no. 7, pp. 1170–1180, 2011.

[47] D. Lee, H. W. Yu, H. Kwon, H.-J. Kong, K. E. Lee, and H. C. Kim, "Evaluation of surgical skills during robotic surgery by deep learning-based multiple surgical instrument tracking in training and actual operations," *Journal of clinical medicine*, vol. 9, no. 6, p. 1964, 2020.

[48] R. L. Achtman, C. S. Green, and D. Bavelier, "Video games as a tool to train visual skills," *Restorative neurology and neuroscience*, vol. 26, no. 4-5, pp. 435–446, 2008.

[49] T. Strobach, P. A. Frensch, and T. Schubert, "Video game practice optimizes executive control skills in dual-task and task switching situations," *Acta psychologica*, vol. 140, no. 1, pp. 13–24, 2012.

[50] P. Richard and P. Coiffet, "Human perceptual issues in virtual environments: sensory substitution and information redundancy," in *Proceedings 4th IEEE International Workshop on Robot and Human Communication*, pp. 301–306, IEEE, 1995.

[51] M. Pieszek, A. Widmann, T. Gruber, and E. Schröger, "The human brain maintains contradictory and redundant auditory sensory predictions," *PLoS One*, vol. 8, no. 1, p. e53634, 2013.

[52] D. M. Wolpert, R. C. Miall, and M. Kawato, "Internal models in the cerebellum," *Trends in cognitive sciences*, vol. 2, no. 9, pp. 338–347, 1998.

[53] J. Huang, A. Isidori, L. Marconi, M. Mischiati, E. Sontag, and W. Wonham, "Internal models in control, biology and neuroscience," in *2018 IEEE Conference on Decision and Control (CDC)*, pp. 5370–5390, IEEE, 2018.

[54] M. Hayhoe, N. Mennie, B. Sullivan, and K. Gorgos, "The role of internal models and prediction in catching balls," in *Proceedings of the american association for artificial intelligence*, pp. 1–5, 2005.

[55] D. M. Wolpert, K. Doya, and M. Kawato, "A unifying computational framework for motor control and social interaction," *Philosophical Transactions of*

the Royal Society of London. Series B: Biological Sciences, vol. 358, no. 1431, pp. 593–602, 2003.

[56] A. J. Bastian, "Learning to predict the future: the cerebellum adapts feedforward movement control," *Current opinion in neurobiology*, vol. 16, no. 6, pp. 645–649, 2006.

[57] A. Kunapareddy and N. J. Cowan, "Recovering observability via active sensing," in *2018 Annual American Control Conference (ACC)*, pp. 2821–2826, IEEE, 2018.